UNIFORMIZING DESSINS AND BELYĬ MAPS VIA CIRCLE PACKING

PHILIP L. BOWERS AND KENNETH STEPHENSON

ABSTRACT. Grothendieck's theory of *Dessins d'Enfants* involves combinatorially determined affine, reflective, and conformal structures on compact surfaces. In this paper the authors establish the first general method for uniformizing these dessin surfaces and for approximating their associated Belyĭ meromorphic functions.

The paper begins by developing a *discrete* theory of dessins based on circle packing. This theory is surprisingly faithful, even at its coarsest stages, to the geometry of the *classical* theory, and it displays some new sources of richness; in particular, algrebraic number fields enter the theory in a new way.

The paper goes on to show that the discrete dessin structures converge to their classical counterparts under a hexagonal refinement scheme. In addition, since the discrete objects are computable, circle packing provides opportunities both for routine experimentation and for large scale explicit computation. A range of examples up to genus 4 is given in the paper, and an appendix addresses implementation issues.

1. INTRODUCTION

We are concerned in this paper with structures on triangulated surfaces. Our motivation is the theory of *Dessins d'Enfants*, traced to Grothendieck [13], an intriguing blend of algebra, combinatorics, conformal geometry, and complex function theory.

The creation mythology of the topic posits a child innocently "drawing" on a topological surface. Unbeknownst (presumably) to the child, that simple drawing determines an algebraic number field and its Galois group, a conformal stucture on the surface, a class of meromorphic functions, and a group of companion drawings. This becomes a story, then, of various rigid algebraic, analytic, and geometric structures, inextricably intertwined, but all flowing from simple combinatorics.

The central aim of the study for algrebraists has been a deeper understanding of the absolute Galois group $\mathrm{Gal}(\overline{\mathbb{Q}}/\mathbb{Q})$ and the famous "inverse Galois problem". Of course, any theory bringing together so many topics will invariably inspire other goals, and an extensive literature has developed. We particularly recommend the proceedings [29] for the 1993 Luminy conference for a broad view. Interests are both theoretical and practical: along with the discussion of "braid towers" and Shimura varieties are the

Date: December 12, 1997.

The second author gratefully acknowledges support of the National Science Foundation and the Tennessee Science Alliance.

efforts of physicists to connect dessins with matrix models in computational studies of Riemann surfaces for string theory.

The authors of the present paper, having worked in circle packing, were drawn to the topic principally through triangulations: combinatorics also lead to rigid geometric structures *via* circle packing. A rich theory has developed around circle packings since their introduction by Thurston in [33] and [34], with particular connections to conformal geometry. One familiar with these developments cannot help but recognize the many parallels with at least the combinatoric and geometric aspects of the theory of dessins. The links promise to enrich the theory and practice of both topics. In addition, there is a visual and numerical side to circle packing which might contribute to the theory of dessins — perhaps introducing an experimental aspect.

To introduce the viewpoint of this paper, it will help to review briefly the elements of the theory of dessins. A *dessin d'enfant* D is basically a finite connected graph on a (compact orientable) surface S. Associated with D is a *canonical triangulation* $\mathcal{T}$ of S; this is our fundamental combinatorial data. A simple genus 0 dessin and its triangulation are given in Figure 1.

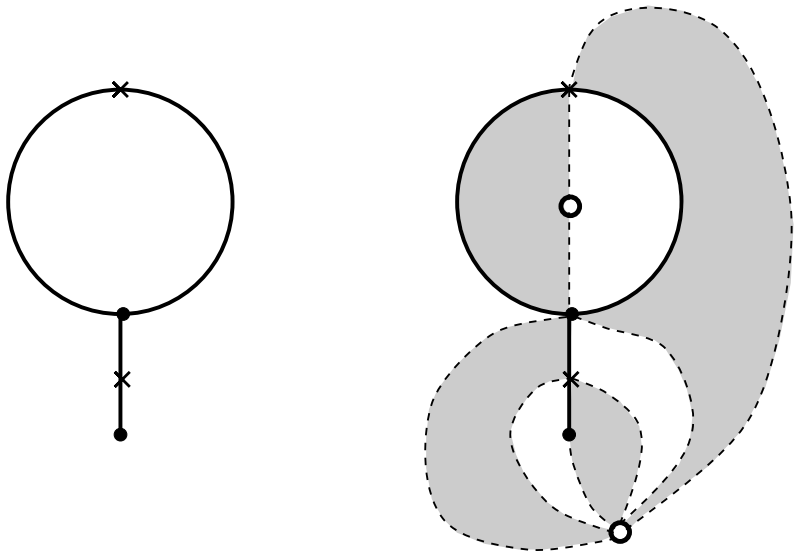

FIGURE 1. A simple dessin and associated triangulation

The triangulation $\mathcal{T}$ in turn imposes a conformal structure on S making it into a Riemann surface S_D; this is accomplished by constructing a model for S by pasting together euclidean unit-sided equilateral triangles in the pattern encoded in $\mathcal{T}$ — a so-called *equilateral surface*. The triangulation is such that alternate faces may be shaded; if the unshaded faces are mapped conformally to the upper half-plane, the

shaded faces to the lower half-plane, and appropriate identifications are made along the intervals $[\infty, 0], [0, 1], [1, \infty]$, then one obtains a meromorphic function $B_D : S_D \longrightarrow \mathbb{S}^2$ branching only over $\{0, 1, \infty\}$. The structures are conveniently packaged in the so-called *Belyĭ pair* (S_D, B_D); indeed, the dessin D itself is in there, being (isomorphic to) the set $B_D^{-1}[0, 1] \subset S_D$. Moreover, the Riemann surface S_D, as an algebraic surface, has a defining equation whose coefficients lie in an algebraic number field F (a finite algebraic extension of the rationals).

For surfaces of positive genus, the results may be summarized in a very striking form. The most difficult of the implications is due to Belyĭ , so this is commonly referred to as

Belyĭ's Theorem. *For a Riemann surface R of genus $g \geq 1$, the following statements are equivalent:*

(a) There exists a defining equation for R whose coefficients lie in an algebraic number field F over the rationals.

(b) There exists a nonconstant meromorphic function $f : R \longrightarrow \mathbb{S}^2$ which branches only over the points $\{0, 1, \infty\}$.

(c) R is conformally equivalent to an equilateral surface.

In other words, we have a distinguished class of Riemann surfaces which simultaneously enjoys algebraic, function-theoretic, and combinatoric characterizations. Equivalent to all these, $R = S_D$ for some dessin D. Thus, all these consequences flow from a simple drawing.

Let us now turn to circle packing and what we will refer to as the "discrete" setting. A **circle packing** is a configuration of circles realizing a specified pattern of tangencies. It enjoys dual combinatoric and geometric natures: the "pattern" of tangencies is encoded as an abstract triangulation of a surface, while circle radii provide the geometry. We paraphrase the central theoretical pivot, with terminology to be explained later.

Theorem. *Let $\mathcal{T}$ be a simplicial triangulation of a compact oriented topological surface S. Then there exists a unique Riemann surface homeomorphic to S that supports a univalent circle packing P with the combinatorics of $\mathcal{T}$.*

Thus circle packings provide an alternate way in which abstract combinatorics determine a rigid conformal structure.

Let's now begin again with a dessin D on a surface S. Generate the associated triangulation $\mathcal{T}$ as before (though for technical reasons we work instead with the barycentric subdivision of $\mathcal{T}$). The Circle Packing Theorem provides a conformal structure for S, giving a Riemann surface, denoted s_D, which supports a circle packing P for $\mathcal{T}$. Again, we may shade alternate faces of $\mathcal{T}$ as defined by the circles. Circles corresponding to the unshaded faces can be identified with circles in the sphere packing the upper half-plane, those corresponding to the shaded faces with circles packing the lower half-plane,

and the edge circles can be appropriately identified along the intervals $[0,1]$, $[1,\infty]$, and $[\infty,0]$ to form a circle packing Q of $\mathbb{S}^2$. The identification of P with Q yields a mapping $b_D : s_D \longrightarrow \mathbb{S}^2$ which acts as a discrete meromorphic function branching only over $0, 1, \infty$. Thus we arrive at a discrete Belyĭ pair (s_D, b_D) associated with our dessin.

In summary, then, a dessin can be associated with rigid conformal data in TWO parallel ways, *via* classical Belyĭ pairs or *via* their discrete analogues.

> ***First Objective:*** *to develop the discrete theory, emphasizing these parallels in combinatorics and geometry.*

However, our discrete objects not only mimic their classical counterparts, but also approximate them. We prove that certain refinements $\mathcal{T}_n$ of a triangulation $\mathcal{T}$, while inducing the identical *classical* Belyĭ pair (S_D, B_D), will lead to new *discrete* Belyĭ pairs $(s_D^{(n)}, b_D^{(n)})$ based on "finer" circle packings. We prove that under successive refinement,

$$(s_D^{(n)}, b_D^{(n)}) \longrightarrow (S_D, B_D), \text{ as } n \to \infty.$$

In other words, the Riemann surfaces $s_D^{(n)}$ converge to S_D in Teichmüller space, while the discrete Belyĭ maps $b_D^{(n)}$ converge uniformly on compacta to B_D. The discrete objects have the advantage that they are effectively computable.

> ***Second Objective:*** *to prove that the objects of the discrete theory generated by circle packings uniformize classical dessin surfaces and approximate classical Belyĭ maps.*

It should be noted that there are varying uses of the term "uniformize" in the dessin literature: For a given dessin surface S_D, this often refers to the structure it inherits from a classical triangle group by modding out a covering group; this is actually a conformal structure on the punctured surface $S_D \backslash V$, where V is the set of vertices of $\mathcal{T}$. On the other hand, we uniformize the full surface S_D. Despite very concrete descriptions of the surfaces, it has been almost impossible to compute such uniformizations in the past, aside from certain highly symmetric situations.

We might exploit the visual nature of circle packings here with an early example — details will come later. Let's consider the dessin of Figure 1. Figure 2(a) illustrates the circle packing of $\mathbb{S}^2$ associated with three stages of refinement of $\mathcal{T}$; the edges of $\mathcal{T}$ are drawn in, with the heavy edges being those of the dessin D, and appropriate faces are shaded. Figure 2(b) illustrates the packings of the upper/lower half planes at the corresponding refinement stage. The discrete meromorphic function $b_D^{(3)}$ identifies each circle on the left with a corresponding circle on the right. (This defines a 4-sheeted covering of $\mathbb{S}^2$, so each circle on the right is the image of four circles on the left.) The discrete dessin is nearly conformally correct, and in positive genus examples, the surface will be nearly equal in modulus to the classical surface. This illustrates our

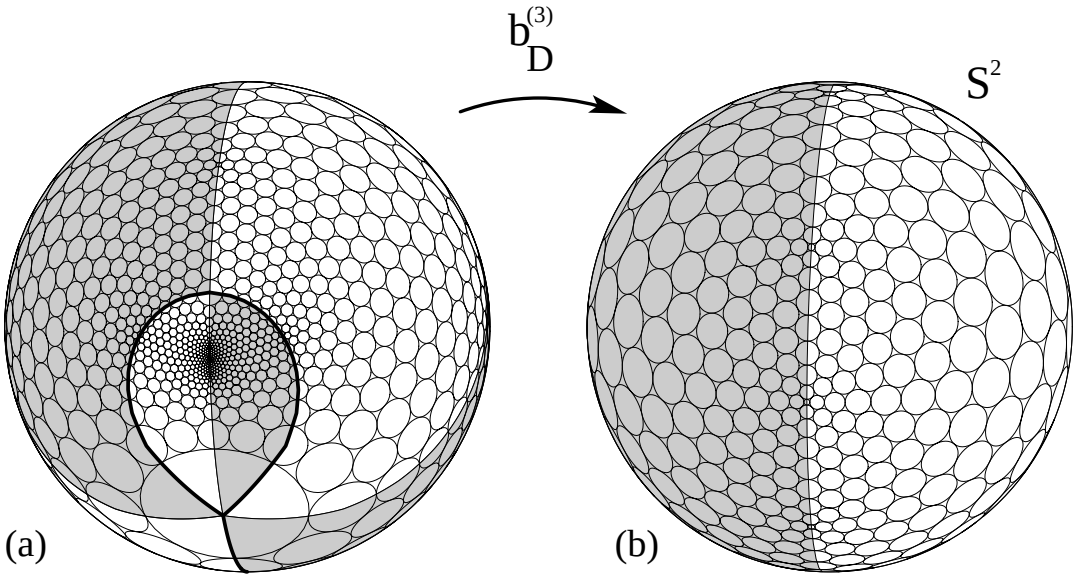

FIGURE 2. A discrete Belyĭ map

Third Objective: *to provide a variety of examples and discuss the computational issues associated with the theory.*

A notable loss in the discrete setting is the direct connection to number fields. Recall that Belyĭ 's Theorem provides an elegant algebraic characterization of the countable dense set of "equilateral" points of Teichmüller space. There is as yet no characterization of the "circle packing" points, also countable and dense; this characterization appears to be a challenging issue. The circle packing points are, of course, *indirectly* associated with number fields *via* the equilateral surfaces. However, it also turns out that algebraic numbers enter directly, but in a new way — as entries in the covering group in $\mathrm{PSL}(2,\mathbb{C})$. There are a number of open questions here, and we will return to this issue in the last section of the paper.

Now for a brief outline of our paper. Section 1 is concerned with dessins in the classical setting (we use the term "classical" only to distinguish it from the discrete setting), and we review the basic terminology, notation, and theory used in the sequel. In Section 2 we develop the parallels in the discrete setting, beginning with the basic theory of circle packing and ending with the discrete Belyĭ pairs.

Section 3 contains the paper's main theoretical results. We introduce the key notions of *reflective structures* and their *conformal subdivisions* for triangulated surfaces. This permits refinement of a triangulation without changing its associated conformal structure. We then prove (Theorems 4.5 and 4.10) that the discrete Belyĭ pairs for

successive refinements of a dessin triangulation converge to the classical Belyĭ pair for the dessin. In other words, using circle packings we simultaneously uniformize the associated Riemann surface and approximate its Belyĭ map.

Section 4 is a Menagerie of examples, organized by genus. We encourage the reader to make an early visit. We illustrate several examples from the dessin literature, classical surfaces such as Klein's and Picard's, and new examples up to genus 4. These show the type and quality of information available in this discrete approach. We discuss computational and experimental issues in Section 5, including a "dessin modification" procedure which, coupled with speedy computation and display, may provide new insights into the behavior of dessins. (For readers wanting more computational details, we have included an Appendix discussing alogrithms, run times, visualization, and so forth. The illustrations in the paper were generated using packages `CirclePack` and `DesPack` available from the second author.)

The paper concludes with a summary of the discrete setting, its faithfulness to its classical counterpart, and directions for further development. This work also raises several questions about circle packing: the characterization of packable Riemann surfaces, the surprising accuracy of even coarse packing structures, and new connections to algebraic numbers.

The authors express their thanks to Jack Quine, Robert Varley, Chuck Collins, and David Singerman for helpful conversations and to Alan Beardon, Keith Carne, and the University of Cambridge for their hospitality during the authors' sabbaticals when this work began.

2. Dessins d'Enfants

Our work involves various procedures for constructing Riemann surfaces (with extra structure) from purely combinatorial data. In this section we review the fundamentals of Grothendieck's theory of *dessins d'enfants* which motivate the developments of the paper. Dessin theory is of recent origin and we refer to it as "classical" only to distinguish it from the coming "discrete" theory.

Authors differ slightly in the terminology they employ for dessins d'enfants. We adopt that of [29, p.4] and refer the reader to [29] for more extensive treatments of the topic and, in particular, for a discussion of the deep and intimate connections between dessins d'enfants, Belyĭ maps, surfaces defined over number fields, and the absolute Galois group $\mathrm{Gal}(\overline{\mathbb{Q}}/\mathbb{Q})$. Here we recall terminology, fix notation, and state results which set the pattern for the remainder of the paper.

2.1. Dessins d'enfants.

Definition. *A **dessin d'enfant**, or **dessin** for short, is an oriented, closed (compact and connected with empty boundary) topological surface S equipped with a finite embedded graph D for which*

1. *the graph D is connected,*
2. *the complement $S\backslash D$ is a (finite) collection of open 2-cells,*
3. *the vertices of D are 2-colorable; i.e., the vertex set V decomposes as the disjoint union of two nonempty collections, V_0 and V_1, such that every edge of D has one vertex in V_0 and the other in V_1.*

Requirement (3) implies that D has no loops, though there may be multiple edges. The vertices in V_i are called the **i-vertices**, for $i = 0, 1$. In diagrams of dessins, we use a solid dot $\bullet$ to mark 0-vertices and a small $\times$ to mark 1-vertices. We consider dessins (S_1, D_1) and (S_2, D_2) to be **equivalent** if there exists an orientation preserving homeomorphism of S_1 to S_2 whose restriction to D_1 is a color-preserving graph isomorphism of D_1 to D_2. We make no distinction between equivalent dessins.

A dessin (S, D), or just D if S is understood from the context, is **pre-clean** if each 1-vertex has valence at most 2 and is **clean** if each 1-vertex has valence equal to 2. There is a standard way to get a clean dessin from a graph G — what Grothendieck described as a "drawing". For simplicity, nearly all our examples will be of this type, although the methods apply to all dessins, and even more general situations. If G is embedded in a surface S and (1) and (2) hold, one obtains a clean dessin D by adding a $\times$ to each edge, so V_0 is the set of original vertices of G and V_1 the set of added vertices. There is no loop-free restriction on the graph G.

By **triangulation** of a surface S we mean a regular cellular decomposition $\mathcal{T}$ of S with each 2-cell a topological triangle so that two 2-cells, when they meet, meet in a subcomplex of the 1-skeleton $\mathcal{T}^{(1)}$. If it happens that two faces can meet only at a single vertex or along a single edge, we refer to $\mathcal{T}$ as a **simplicial triangulation** of S. In general, however, a triangulation might have faces meeting along the union of

two sides, along one common side and a common opposite vertex, along three common vertices but no sides, or even along all three sides. Notice that we view a triangulation as a structure *in situ*, as a collection of actual subsets of S — vertices consisting of points of S, edges consisting of arcs in S, and faces consisting of 2-cells in S. Abstract triangulations — purely combinatorial objects — will always have surfaces as geometric realizations. The **degree** of a triangulation is the maximum of the degrees of its vertices; that is, the largest number of edges emenating from any one vertex.

Associated with a dessin (S, D) is a **canonical triangulation** of S, denoted $\mathcal{T} = \mathcal{T}(D)$, described as follows. The vertex set of $\mathcal{T}$ is the disjoint union $V_0 \cup V_1 \cup V_\infty$, where V_0 and V_1 are as before and V_∞ consists of a collection of points from $S \backslash D$, one point from each (2-cell) component of $S \backslash D$. The edges of $\mathcal{T}$ consist of the edges of D along with edges formed by connecting vertices in $V_0 \cup V_1$ with those of V_∞ as follows. For $v \in V_0 \cup V_1$, let Δ be a disc neighborhood of v that meets D only at points of $\mathrm{st}(v, D)$; i.e., at points in the edges of D incident with v. The edges of D divide Δ into d open sectors, where $d = \deg(v, D)$. Add, for each sector Σ, an edge emanating from v, meeting D only at v, and traveling along an arc through Σ into the 2-cell component of $S \backslash D$ containing Σ until it meets the vertex in V_∞ in that component. We proceed, of course, so that new edges, if they meet, meet only at the vertices in V_∞. For the general dessin on the left in Figure 1, the procedure produces the cellular decomposition of $S = \mathbb{S}^2$ on the right. As we shall do subsequently, we have marked the **∞-vertices**, the elements of V_∞, with open dots $\circ$. The open faces of $\mathcal{T}$ consist of the components of $X \backslash \overline{E}$, where $\overline{E}$ denotes the union of the edges of $\mathcal{T}$. Notice that each face of $\mathcal{T}$ is a topological triangle with three vertices, one of each type, and a circuit of three edges, one of type $\bullet$——$\times$, one of type $\bullet$——$\circ$, and another of type $\times$——$\circ$. The faces are naturally partitioned into two collections by the orientation on S, depending on whether or not the circuit $\circ$——$\bullet$——$\times$——$\circ$ around the boundary of a face is compatible with the orientation the face inherits from the orientation of S. If the circuit $\circ$——$\bullet$——$\times$——$\circ$ is compatible, we call the face a $(+)$triangle; otherwise a $(-)$triangle. In diagrams, we shall shade in the $(-)$triangles, as in Figure 1. Notice that each vertex of $\mathcal{T}$ has even degree, and no two $(+)$triangles (resp. $(-)$triangles) share a common edge. Any two canonical triangulations of (S, D) are not only combinatorally equivalent, but isotopic, so we may speak of **the** canonical triangulation of (S, D).

2.2. **The Equilateral Structure.** Up to this point, a dessin represents purely combinatorial data. However, it can be realized geometrically as a piecewise equilateral surface.

Definition. *Let $\mathcal{T}$ be a triangulation of the topological surface S (possibly with boundary). An **equilateral metric structured on $\mathcal{T}$** is a piecewise euclidean distance function on S in which each edge of $\mathcal{T}$ is isometric with the unit interval $[0, 1]$ and each face of $\mathcal{T}$ is isometric with a euclidean unit equilateral triangle. The surface S equipped with such a metric is termed an **equilateral surface structured on $\mathcal{T}$**, and is denoted as $|\mathcal{T}|_{eq}$.*

One can always construct such a metric, defining it first on the 1-skeleton, extending locally so that each face becomes a euclidean unit equilateral triangle, and finally defining the distance between points as the length of a shortest path between them, which always exists. We could equally well use edges of length $\varepsilon > 0$, in which case we denote the surface by $|\mathcal{T}|^{\varepsilon}_{eq}$; this simply respresents a scaling of the metric by ε.

One next defines a compatible conformal structure. Each edge $e \in \mathcal{T}$ is shared by two faces $f_{\pm}$; let $U_e \subset S$ denote the open set $f_+^\circ \cup e^\circ \cup f_-^\circ$. Define $\Omega \subset \mathbb{C}$ to be the interior of the union $\triangle \cup \overline{\triangle}$, where $\triangle$ is a unit equilateral triangle with vertices $\langle 0, 1, \frac{(1+\sqrt{3}i)}{2} \rangle$. From the definition of our equilateral metric, it is evident that there exists an orientation-preserving, isometric map φ_e of U_e onto Ω. The charts $\{(U_e, \varphi_e) : e \in \mathcal{T}\}$ provide $S \backslash V$, where V is the vertex set of $\mathcal{T}$, with a covering by compatible analytic charts determining a complex atlas. This atlas can be augmented by introducing charts involving appropriate power functions in neighborhoods of the isolated singularities at the vertices V (see, e.g., [3, §3.3]). The resulting atlas defines a conformal structure for all of S.

Definition. *In general, if $\mathcal{T}$ is a triangulation of a topological surface S, the Riemann surface associated with the equilateral surface structured on $\mathcal{T}$ is called the* ***equilateral surface*** *for $\mathcal{T}$ and denoted $S_{\mathcal{T}}$. In case $\mathcal{T} = \mathcal{T}(D)$, the canonical triangulation for dessin D, we refer to this Riemann surface as the* ***dessin surface*** *and denote it by S_D.*

Note that $\mathcal{T}$ will be treated as an *in situ* triangulation of $S_{\mathcal{T}}$. As such, it is uniquely determined up to conformal automorphisms and will be treated as fixed; when necessary, a convenient normalization may be imposed. We will be investigating the "reflective" nature of these structures in the sequel.

2.3. **The Belyĭ Map.** A **Belyĭ map** of a Riemann surface R is a meromorphic function $B : R \longrightarrow \mathbb{S}^2$ that is ramified only over 0, 1, and ∞. (In other words, if B fails to be locally one-to-one at a point $z \in R$, then $B(z)$ equals $0, 1$, or ∞.)

Using Schwarz reflection, one constructs a canonical Belyĭ map for a given dessin surface S_D as follows. A dessin face $f \in \mathcal{T}(D)$ is a topological triangle with a conformal structure inherited from S_D; consequently there exists a unique conformal mapping of the interior of f onto an open hemisphere of $\mathbb{S}^2$ that extends continuously to ∂f and carries the j-vertex to $j \in \mathbb{S}^2$, $j = 0, 1, \infty$. Orientation guarantees that $(+)$triangles are mapped to the upper half-plane, $(-)$triangles to the lower. Define B on the interior of each face f to be the associated conformal map. If faces $f_{\pm}$ share an edge e of $\mathcal{T}(D)$, recall the map $\varphi_e : U_e \longrightarrow \Omega$ defined above. If $g = B \circ \varphi_e^{-1}$, then the restriction of g to $\triangle \subset \Omega$ (resp. $\overline{\triangle} \subset \Omega$) is a conformal map onto the upper (resp. lower) half-plane and g extends to the interval $[0, 1]$ and is real there. By Schwarz reflection, g extends analytically to a conformal map on all of Ω. In particular, then, B extends analytically across the open edge e and is locally one-to-one. That is, B is a smooth analytic covering map of $S_D \backslash V$ onto the thrice punctured sphere $\mathbb{S}^2 \backslash \{0, 1, \infty\}$. The

isolated singularities are removable, with values in $\{0, 1, \infty\}$ so B is a meromorphic function on S_D which can branch only over $\{0, 1, \infty\}$.

Definition. *Given a dessin (S, D), the meromorphic function $B : S_D \longrightarrow \mathbb{S}^2$ defined as above is termed the* ***Belyĭ map for*** *D and will be denoted B_D. Note that B_D is uniquely determined up to conformal automorphisms of S_D. The pair (S_D, B_D) is called a (classical)* ***Belyĭ pair****. The set $B_D^{-1}[0, 1] \subset S_D$ is D and in the presence of the conformal structure will be called a* ***conformally correct*** *dessin.*

Note that any pair (R, B), where R is a compact Riemann surface and $B : R \longrightarrow \mathbb{S}^2$ is a Belyĭ map, will be a Belyĭ pair for the dessin $D = B^{-1}[0, 1] \subset R$.

In summary, then, the classical theory takes one from elementary and purely combinatorial data to a rigid geometric surface and an explicit associated meromorphic function. Recall that Belyĭ 's Theorem further associates with each Belyĭ pair an algebraic number field; we will not make direct use of this.

3. Discrete Dessins *via* Circle Packing

In this section we develop the discrete parallels of the classical objects in the previous section. First we review the background on circle packings pertinent to our task of uniformization; the basic references for this material are [4, 7, 10, 14, 24, 28, 31, 33]. For background on Riemann surfaces, see [3, 11].

3.1. Circle Packings.

Circle packings are configurations of circles realizing specified patterns of tangency. The key to understanding them lies in recognizing their dual natures, *geometric* in the radii of the circles, but *combinatoric* in their required pattern of contact. We first discuss geometry on Riemann surfaces, then the encoding of the combinatorics.

Recall that every Riemann surface admits an essentially unique complete metric of constant curvature 0 or ± 1 that is compatible with its conformal structure in the very strong sense that isothermal local coordinates determined by the metric cover the surface with analytic charts from the complete complex atlas of the surface [35]. This metric will be termed an **intrinsic metric** for the surface and is unique up to isometry. One of the most useful properties of an intrinsic metric is that it is **conformal**, meaning that the angle between two smooth curves on the surface that is determined by the Riemannian metric agrees with the angle determined by any appropriate chart in the complex atlas of the surface.

Let ρ be an intrinsic metric for the Riemann surface R. A metric disk in R of radius $r > 0$ and center $z \in R$ is a topological 2-cell D in R for which

$$D = \{w \in R : \rho(z, w) \leq r\}.$$

The boundary of D, $\partial D = \{w \in R : \rho(z,w) = r\}$, is then a topological circle and is said to be a metric circle in R with center z. The term **circle** will always refer to a metric circle in the intrinsic metric of the appropriate Riemann surface.

All our circle packings will be associated with triangulations. More formally, suppose $\mathcal{K}$ is an abstract simplicial 2-complex that triangulates an orientable topological surface; we use the abbreviated term **complex**. A configuration P of circles in a Riemann surface R is a **circle packing for** $\mathcal{K}$ provided (i) P contains a circle c_v associated with each vertex $v \in \mathcal{K}^{(0)}$, (ii) c_v is (externally) tangent to c_w at a single point whenever vw is an edge of $\mathcal{K}$, and (iii) the geodesic segments connecting the centers of c_u, c_v, and c_w bound a metric triangle in R whenever uvw is a face of $\mathcal{K}$. The geometric 2-complex in R determined by connecting centers of tangent circles in P by geodesic segments is called the **carrier** of P, written $\mathrm{carr}(P)$.

In this paper, P will always be **univalent**, meaning that the circles have mutually disjoint interiors, and $\mathrm{carr}(P)$ fills R. In this case, $\mathrm{carr}(P)$ provides a concrete realization of the abstract complex $\mathcal{K}$ as a geodesic triangulation of the surface R, each face a metric triangle with geodesic sides. Considerably more striking is the fact that the abstract complex $\mathcal{K}$ actually determines uniquely the Riemann surface R; this is the content of the following basic existence-uniqueness result, a proof of which may be found in [4, 33]. We state the result for compact orientable surfaces.

Circle Packing Theorem. *Let $\mathcal{K}$ be an oriented abstract simplicial complex triangulating a compact, connected, oriented topological surface S. Then S admits uniquely the structure of a Riemann surface R that supports a univalent circle packing P for $\mathcal{K}$ respecting the orientations; moreover, the circle packing P is unique up to conformal automorphisms of R.*

If $\mathcal{K}$ and S are as in the Circle Packing Theorem, the Riemann surface R will be denoted by $|\mathcal{K}|_{cp}$ and the packing P, with circles measured in the intrinsic metric of $|\mathcal{K}|_{cp}$ (constant curvature 0, ± 1), will be denoted $P_{\mathcal{K}}$. We call $|\mathcal{K}|_{cp}$ the **circle packing surface** determined by $\mathcal{K}$ and refer to its conformal structure as a **discrete** conformal structure; it is a perfectly legitimate conformal structure, the adjective "discrete" simply acknowledges its source. When S has genus 0, then $|\mathcal{K}|_{cp}$ is the Riemann sphere; an additional normalization of $P_{\mathcal{K}}$ will typically be necessary, since circle radii and centers (and hence $\mathrm{carr}(P_{\mathcal{K}})$) are not invariant under conformal automorphisms.

Circle packings exist in great variety, and mappings among them have been shown to display quantitative and qualitative properties associated with analytic functions. Indeed, the proof of the Circle Packing Theorem follows closely the lines of classical covering theory and the Riemann Mapping Theorem. We require only parts of this broader theory.

Let's begin with covering theory. A complex $\mathcal{K}$ triangulating a compact orientable surface S can always be "lifted" to a simply connected complex $\widetilde{\mathcal{K}}$ triangulating the universal covering surface of S. The Discrete Uniformization Theorem of [4] gives

an essentially unique **maximal** univalent circle packing $\widetilde{P}$ for $\widetilde{\mathcal{K}}$. If $\widetilde{\mathcal{K}}$ is finite, then $\widetilde{\mathcal{K}} = \mathcal{K}$, $\widetilde{P} = P$ packs the Riemann sphere, and we are finished. Otherwise, $\widetilde{P}$ is an infinite packing whose carrier is either the euclidean or the hyperbolic plane. If we denote this plane by $\mathcal{D}$, then $\widetilde{P}$ is unique up to elements of $\mathrm{Aut}(\mathcal{D})$, the conformal automorphisms (Möbius transformations) of $\mathcal{D}$. The simplicial deck transformations of the abstract covering $\widetilde{\mathcal{K}} \longrightarrow \mathcal{K}$ are identified with a discrete group , $\subset \mathrm{Aut}(\mathcal{D})$ which leaves $\widetilde{P}$ invariant. Therefore, $\widetilde{P}/$, may be identified with a circle packing P for $\mathcal{K}$ in the Riemann surface $R = \mathcal{D}/$, . Even the radii are unaffected by this identification, since the intrinsic metric of R is precisely that inherited from the metric of $\mathcal{D}$. When we come to examples in our Menagerie, the only practical way to display packings of surfaces is to identify them with fundamental domains within their universal covering packings.

Next, let us consider maps between circle packings, the identification map $\widetilde{P} \longrightarrow \widetilde{P}/$, $= P$ being a prime example. In general, let P and Q be circle packings lying in (possibly distinct) Riemann surfaces. A map $f : P \longrightarrow Q$ which preserves tangencies and orientation is termed a **discrete analytic function**; if Q lies on the Riemann sphere, f is called a **discrete meromorphic** function, and we will see examples of these shortly. The projection $\pi : \widetilde{P} \longrightarrow \widetilde{P}/$, is a **discrete covering map**. The map f clearly induces a simplicial map of $\mathrm{carr}(P)$ to $\mathrm{carr}(Q)$. We will abuse notation and use f to denote both the set map $f : P \longrightarrow Q$ and the associated point mapping $f : \mathrm{carr}(P) \longrightarrow \mathrm{carr}(Q)$ defined to carry the center of each circle $c \in P$ to the center of $f(c) \in Q$ and then extended *via* barycentric coordinates. The function f is basically a simplicial map which acquires the geometry imposed by the circle packings of its domain and range.

Remark. Natural barycentric coordinates for geodesic triangles exist in each of our classical geometries; in the hyperbolic setting, they are most easily described in the hyperboloid model, where geodesics are the intersections of planes through the origin with the hyperboloid sheet (see [35, 27]). In particular, as a point mapping, f is a continuous, orientation preserving, light interior mapping of $\mathrm{carr}(P)$. It maps each edge of $\mathrm{carr}(P)$ "convexly" onto an edge of $\mathrm{carr}(Q)$ in the metric sense. We will see later that lower bounds on the angles of the faces in $\mathrm{carr}(P)$ and $\mathrm{carr}(Q)$ also give bounds on the quasiconformal dilitation of f on the interiors of the faces.

Discrete analytic functions can fail to be locally one-to-one, even between univalent packings. Consider $f : P \longrightarrow Q$ with P and Q univalent. Let $c_0 \in P$; the flower of c_0 consists of c_0 as the **center** and the sequence $\{c_1, c_2, \cdots, c_k\}$ of petal circles. The petals are tangent to c_0, successively tangent to one another, and wrap around c_0 once in the positive direction. The image circles $\{f(c_1), f(c_2), \cdots, f(c_k)\}$ in Q will necessarily be petals of the flower of $f(c_0)$. By orientation they must wrap in the positive direction about $f(c_0)$; if they wrap $n \geq 2$ times around $f(c_0)$, we say that f has a (discrete) **branch point** at c_0 of **order** $n-1$. For instance, if 12 "petals" around c_0 are mapped

to four about $f(c_0)$, the result is a branch point of order 2, with each petal of $f(c_0)$ the image of three petals of c_0.

Those curious about the practical side of circle packing should see the Appendix, which briefly discusses numerical algorithms, implementation, and software. For further connections between circle packing and analytic functions, see [4, 10, 28] and references therein.

3.2. **Discrete Dessins.** Suppose that a fixed dessin (S, D) is given. We are now in position to create its associated discrete Belyĭ pair.

Recall that the canonical triangulation $\mathcal{T} = \mathcal{T}(D)$ may not be simplicial. For this and several other practical reasons we perform a barycentric subdivision of $\mathcal{T}$ and denote the resulting complex by $\mathcal{K} = \mathcal{K}(D)$.

Definition. *Given a dessin (S, D), the Circle Packing Theorem implies existence of the Riemann surface $|\mathcal{K}(D)|_{cp}$, homeomorphic to S, supporting a circle packing $P_{\mathcal{K}}$ for $\mathcal{K}$. We denote this Riemann surface by s_D and refer to it as the* ***coarse circle packing surface*** *for D and refer to the packing $P_{\mathcal{K}(D)}$ as the* ***coarse circle packing*** *P_D.*

Observe that $\mathcal{T}$ is represented in $\mathcal{K}$: its 0-, 1-, and ∞-vertices are among the vertices of $\mathcal{K}$; each edge of $\mathcal{T}$ is a chain of edges (at this stage, two) of $\mathcal{K}$; and each "dessin" face is now a union of faces (six) of $\mathcal{K}$. Thus s_D constitutes the "surface" part of a discrete Belyĭ pair and provides a geometry for $\mathcal{T}$. When s_D is the Riemann sphere, a normalization of P_D is needed. For this purpose, we will designate 0-, 1-, and ∞-vertices v_0, v_1, v_∞ of $\mathcal{T}$ and apply an automorphism to ensure that these points of $\mathrm{carr}(P_D)$ are located at $0, 1$, and ∞, respectively, on $\mathbb{S}^2$.

For the meromorphic function part we must first describe the standard coarse circle packing Q for the Riemann sphere: Choose three points on a topological circle on a topological sphere; this breaks the circle into three segments and defines a triangulation $\mathcal{T}$ of the sphere, the two faces sharing a common boundary. Its barycentric subdivision $\beta\mathcal{T}$ will be denoted by $\mathcal{H} = \mathcal{H}_0$ and defines an abstract simplicial triangulation of the topological sphere. The Circle Packing Theorem guarantees a packing Q for $\mathcal{H}$ on the Riemann sphere $\mathbb{S}^2$. This Q is shown on the right in Figure 3, with a normalization placing the vertices of $\mathcal{T}$ at $0, 1, \infty$ and with shading of the triangle of $\mathcal{T}$ (six faces of $\mathcal{H}$) forming the lower half-plane. (Our conventional orientation of $\mathbb{S}^2$ in $\mathbb{R}^3$ means that the "lower" half-plane is the left hemisphere.)

We are now in position to define a discrete meromorphic function $b_D : P_D \longrightarrow Q$. The vertices of $\mathcal{T}$ have been decomposed into sets V_0, V_1, and V_∞. Identify each circle associated with a 0-vertex to the circle of Q centered at 0, each 1-vertex to the circle of Q centered at 1, and each ∞-vertex to the circle of Q centered at ∞. Tangencies and orientation clearly dictate that the seven circles of P_D defining any $(+)$triangle of $\mathcal{T}$ are carried to the seven circles of Q forming the unshaded upper half-plane, while the seven forming any $(-)$triangle are carried to the seven forming the shaded lower half-plane.

Definition. *Given a dessin (S, D), the associated* ***coarse discrete Belyĭ pair*** *is the pair (s_D, b_D) consisting of the coarse circle packing surface for D and the discrete meromorphic function $b_D : S_D \longrightarrow \mathbb{S}^2$.*

The coarse pair for the simple dessin of Figure 1 is illustrated in Figure 3. The surface s_D is just $\mathbb{S}^2$ in this genus 0 case, but the locations of its vertices are determined by the packing P_D, and these define the dessin itself, shown with the thick line.

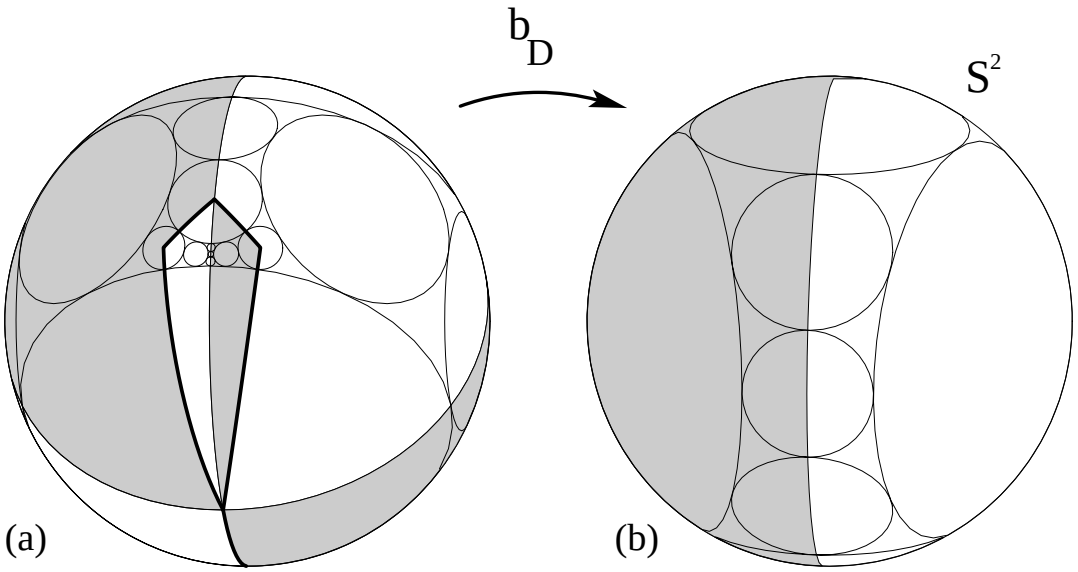

FIGURE 3. A coarse discrete Belyĭ pair

All nontrivial discrete Belyĭ maps will have branch points. For instance, Figure 3 is associated with the dessin of Figure 1; it has an ∞-vertex which belongs to 6 faces of $\mathcal{T} = \mathcal{T}(D)$, alternately $(+)$ and $(-)$triangles. These six are mapped by b_D to the two triangles forming the upper and lower half-planes, respectively, in Q; consequently, this ∞-vertex is a branch point of order two for b_D. This behavior, mimicking the classical situation, is typical: a dessin vertex v which belongs to $2n$ faces of $\mathcal{T}$ engenders a branch point of order $n-1$ in the Belyĭ map. Moreover, one can easily check that b_D does not branch at vertices of $\mathcal{K}$ which are not dessin vertices (i.e., vertices of $\mathcal{T}$). In a clean dessin, all the 1-vertices are simple branch points (order 1).

It is important to recognize that the discrete Belyĭ pair (s_D, b_D) and the classical Belyĭ pair (S_D, B_D) are *qualitatively* indistinguishable. The surfaces s_D and S_D are homeomorphic to one another, since each is homeomorphic to the topological surface S. In fact there exist homeomorphisms $\phi : S \longrightarrow s_D$ and $\Phi : S \longrightarrow S_D$ which respect the embedded $\mathcal{T}$'s. The maps $s_D \circ \phi : S \longrightarrow \mathbb{S}^2$ and $S_D \circ \Phi : S \longrightarrow \mathbb{S}^2$ are open, continuous, orientation preserving maps sharing valence and branch structures. In

fact, $s_D \circ \phi$ and $S_D \circ \Phi$ are isotopic maps. Topologically and combinatorially, these pairs can't be distinguished.

3.3. **Hexagonal Refinement.** The discrete objects created so far are termed "coarse" only because they involve so few circles for carrying the geometric information. There is a rule-of-thumb in circle packing: *the finer the circle packing, the closer its geometric behavior to classical conformal behavior.* So we need packings with more numerous and smaller circles if we hope to approach continuous behavior. We deploy a process called hexagonal-refinement.

We use α to indicate the **hex subdivision** operator which, when applied to a complex $\mathcal{K}$ triangulating a surface S, yields the complex $\alpha\mathcal{K}$ also triangulating S. Its effect is illustrated in Figure 4: one first adds a vertex to the middle of each edge of $\mathcal{K}$ and then adds three edges in each face of $\mathcal{K}$ to connect pairs of the new vertices. Thus, each triangle (face) of $\mathcal{K}$ is broken into four triangles in $\alpha\mathcal{K}$. The vertices of $\mathcal{K}$ remain, with their degrees unchanged; each new vertex, being in the edge of two faces, has degree six, hence the adjective "hexagonal". Repeated applications will be indicated with powers, $\alpha^n\mathcal{K}$; three stages of hex refinement of a triangle are shown in the figure.

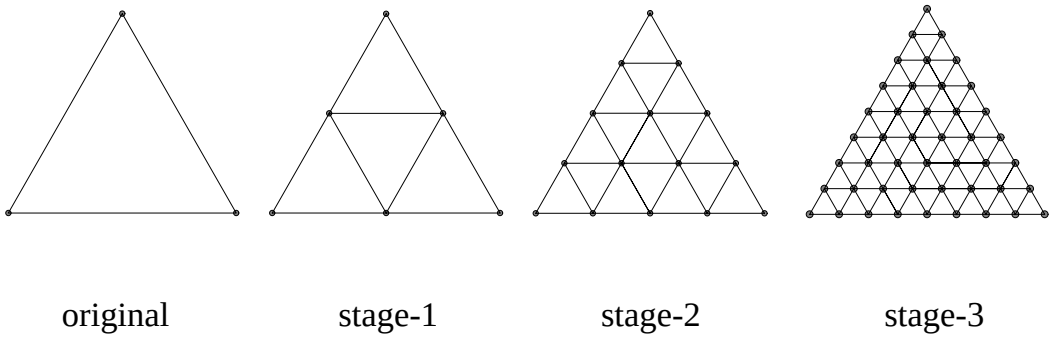

FIGURE 4. The hexagonal subdivision operation

In the case of a dessin (S, D), we have the complex $\mathcal{K} = \beta\mathcal{T}$ triangulating S, the complex $\mathcal{H}$ triangulating the sphere, and the coarse discrete Belyĭ map $b_D : P_D \longrightarrow Q$ between their packings. We simply hex refine $\mathcal{K}$ and $\mathcal{H}$, obtain circle packings for the refinements, and arrive at a "refined" map between them.

In particular, by the Circle Packing Theorem, there is a Riemann surface $|\alpha\mathcal{K}|_{cp}$ homeomorphic to S which supports a circle packing for $\alpha\mathcal{K}$; denote the Riemann surface by $s_D^{(1)}$ and the packing by $P_D^{(1)}$. Likewise, there is a circle packing on $\mathbb{S}^2$ for the refinement $\alpha\mathcal{H}$, to be denoted $Q^{(1)}$ and normalized to keep the original three vertices at $0, 1, \infty$, respectively. It is elementary to see that b_D, as a simplicial map between $\mathcal{K}$

and $\mathcal{H}$, induces a simplicial map between $\alpha\mathcal{K}$ and $\alpha\mathcal{H}$; in fact, on the vertex set, the new map extends the original. This defines the circle packing map from $P_D^{(1)}$ to $Q^{(1)}$ which we denote by $b_D^{(1)}$. We therefore arrive at a new discrete Belyĭ pair $(s_D^{(1)}, b_D^{(1)})$. We may repeat this refinement process any finite number of times.

Definition. *Given a dessin (S, D) and $n \geq 0$, the* ***stage-n discrete Belyĭ pair*** *associated with (S, D) is the pair $(s_D^{(n)}, b_D^{(n)})$ obtained from the coarse pair (s_D, b_D) by n successive stages of hexagonal refinement and repacking. The associated stage-n circle packing of $s_D^{(n)}$ is $P_D^{(n)}$, the stage-n packing of the sphere is $Q^{(n)}$, so $b_D^{(n)} : P_D^{(n)} \longrightarrow Q^{(n)}$.*

It will be a standing assumption in the genus 0 case that $P_D^{(n)}$ has been normalized as follows: for each $i \in \{0, 1, \infty\}$ an i-vertex v_i has been designated; a Möbius transformation has been applied to the sphere so that vertex v_i of $\mathrm{carr}(P_D^{(n)})$ is located at i, for $i = 0, 1, \infty$.

A stage-n discrete Belyĭ pair will again be *qualitatively* indistinguishable from the other stages and from the classical Belyĭ pair. In particular, the branch points of $b_D^{(n)}$ occur at dessin vertices (the original vertices inherited from $\mathcal{T}$) and branch orders are preserved under refinement (because degrees of vertices are preserved). The $b_D^{(n)}$ have identical branch structures, and, as maps from S to $\mathbb{S}^2$, will be isotopic to one another. One would expect the pairs to be distinct, however, in their *quantitative* structure. A packing $P_D^{(n+1)}$ is not a direct "refinement" of $P_D^{(n)}$ (no one has discovered a good way to refine circle packings as one could, say, squares), only the *combinatorics* are being refined. In fact, there is, in the absense of special symmetries, no reason to expect the Riemann surfaces $s_D^{(n+1)}$ and $s_D^{(n)}$ to be conformally equivalent; in other words, the geometries are different.

Figure 2 in the Introduction is the stage-3 discrete Belyĭ pair associated with the coarse pair of Figure 1. It is intuitively clear that finer packings will carry more geometric information than their coarser predecessors. We make this very precise in Section 4.

3.4. **Geometric Lemmas.** The bounded geometry associated with circle packings is critical to our uniformization work. It is a standard feature of the theory dating from the seminal work of Rodin and Sullivan. In the following, (S, D) is our dessin, as usual; however, the results apply equally well to the more general triangulations of the next section. Here, $d = \max\{6, \deg(\mathcal{K})\} = \deg(\mathcal{K}_n), n \geq 1$.

The bounded geometry enters primarily through the Ring Lemma [28].

Lemma 3.1. *There exists a constant $\Theta = \Theta(d) > 0$, depending only on d, so that the following holds: If S has positive genus, then the angles of the faces of* $\mathrm{carr}(P_D^{(n)})$ *are bounded below by Θ for all $n \geq 0$. If S has genus 0, then these angles are bounded below by Θ for n sufficiently large.*

Proof. In the euclidean case, the Ring Lemma tells us that in a univalent packing, the ratio of the radii of two neighboring (interior) circles is bounded by a constant

depending only on degree. This easily converts to a lower bound on angles of faces in the carrier, since they are formed by triples of neighboring circles. The arguments extend easily to cover the hyperbolic setting.

On the sphere, however, the Ring Lemma fails; the ratio of radii for neighbors may be made arbitarily large by applying a suitable Möbius transformation to the packing. Our normalization becomes crucial: we show in Lemma 3.4 below that for sufficiently large n, the spherical radii of circles of $P_{\mathcal{K}_n}$ will be bounded by $\pi/6$. In particular, any flower of circles will lie in a hemisphere. Stereographic projection of that hemisphere to the plane, application of the euclidean Ring Lemma, and some elementary geometry shows that the angles of faces of $\mathrm{carr}(P_D^{(n)})$ will be bounded below by a positive constant depending only on d. □

To convert the bounded geometry of packings to the distortion of associated maps, we need this geometric lemma, whose proof is standard. References to the literature on quasiconformal maps will be given in the next section.

Lemma 3.2. *Let T and T' be geodesic triangles, each lying in the sphere, the euclidean, or the hyperbolic plane. Assume $\theta > 0$ is a lower bound for the angles of T and for the angles of T', measured in their respective geometries. Then the barycentric map $g : T \longrightarrow T'$ is κ-quasiconformal for a $\kappa \geq 1$ depending only on θ.*

Recall that as point mappings, the discrete Belyĭ map $b_D^{(n)}$ carries faces of $\mathrm{carr}(P_D^{(n)})$ barycentrically onto faces of $\mathrm{carr}(Q^{(n)})$. By Lemmas 3.1 and 3.2, the restriction of $b_D^{(n)}$ is κ-quasiconformal on open faces. By removability of analytic arcs and isolated singularities, $b_D^{(n)}$ is κ-quasiregular. In conclusion, we have the following:

Proposition 3.3. *There exists a constant $\kappa = \kappa(d) > 1$ depending only on d so that the following holds: If S has positive genus, then $b_D^{(n)} : s_D^{(n)} \longrightarrow \mathbb{S}^2$ is κ-quasiregular for all $n \geq 0$. If S has genus zero, then $b_D^{(n)}$ is κ-quasiregular for all sufficiently large n.*

Our last result of the section relies on the Rodin and Sullivan Length-Area Lemma along with the Ring Lemma. It confirms one's intuition that the radii of circles in refined packings should go to zero. We actually require only the genus 0 case in this paper (for use in the proof of Lemma 3.1 above). However, the idea of the proof easily generalizes and may be useful in other circumstances.

When S has genus 0, we require the standard normalization of packings noted earlier. When S has genus 1, the euclidean metric of $s_D^{(n)}$ is determined only up to a scalar, so we may assume that $\mathrm{diam}(s_D^{(n)}) = 1$. No normalization is needed when S has genus greater than one.

Lemma 3.4. *Let r_n be the maximum radius among the circles of the normalized packing $P_D^{(n)}$. Then $r_n \longrightarrow 0$ as $n \to \infty$.*

Proof. We begin on the sphere. Everything follows from very local considerations, so fix a vertex v of $\mathcal{T}$. Let γ denote the simple closed edge-path in $\mathcal{K}$ running through the

neighbors of v. In $\mathcal{K}$, this path separates v from at least two of the three designated vertices v_0, v_1, v_∞ used in the normalization of the packings. Without loss of generality, assume γ separates v from v_1 and v_∞.

As $\mathcal{K}$ is *hex* refined, the new complexes $\mathcal{K}_n$ have additional chains of vertices layered between v and γ (which is also refined); in a sense, this region combinatorially "fattens" as n grows. For each n let p_n denote the collection of circles from $P_D^{(n)}$ corresponding to vertices of $\mathcal{K}_n$ separated from 1 and ∞ by γ and let p_n' be the same collection with the circle $c_{v,n}$ for v removed. Observe that the combinatorics of p_n' depend only on d and n; it is a combinatorial annulus of particularly simple type which we describe below. If $A_n \subset \mathbb{S}^2$ denotes the annulus bounded by $\partial c_{v,n}$ and γ, then $p_n' \subset A_n$. Below we will use p_n' to establish a lower bound M_n on the modulus of A_n which goes to infintiy with n. In other words, $c_{v,n}$ is seen to be separated from 1 and ∞ on $\mathbb{S}^2$ by an annulus whose modulus goes to ∞ with n. We may conclude by standard arguments about extremal annuli that the spherical radius of $c_{v,n}$ must go to zero, with rate governed by d. This will conclude the genus 0 case.

Since we don't have the Ring Lemma on the sphere, we project p_n' to the plane. Observe that the circles of p_n' break naturally into n disjoint chains of circles. Let the corresponding edge-paths be denoted $\gamma_1, \gamma_2, \cdots, \gamma_n$, ordered so that γ_j separates v from γ_{j+1}. Let $l_1, l_2, \cdots, l_{n+1}$ denote the combinatorial lengths of these paths. γ_1 is just the edge-path through the neighbors of v in $\mathcal{K}_n$, so $l_1 = \deg(v, \mathcal{K}) \leq d$. We obtain easy bounds on the successive combinatorial lengths because these vertices, all resulting from *hex* refinement, are of degree six. In particular, one can show that $l_j \leq j, j = 1, \cdots, n$. That allows us to write down the quantity pertinent to the Length-Area Lemma, ([28, p. 353]); namely define $k_n = k_n(d)$ by

$$k_n(d) = [\frac{1}{d}(1 + \frac{1}{2} + \frac{1}{3} + \cdots + \frac{1}{n})]^{-1/2} \geq [\frac{1}{l_1} + \frac{1}{l_2} + \cdots + \frac{1}{l_n}]^{-1/2}.$$

Since the harmonic series diverges, k_n goes to zero as n grows.

The argument of the Length-Area Lemma is only indirectly about moduli of ring domains; we need to do some adjustment. First, stereographically project p_n (which avoids ∞) to a packing q_n of the plane. Repack q_n as a "maximal" or Andreev packing $\widehat{q}_n$ in $\mathbb{D}$ with the circle c corresponding to v at the origin (see [4]). The chains of circles associated with the γ_j in p_n now correspond to chains of circles separating c from the boundary of the unit disc. By the argument in the proof of the Length-Area Lemma, radius$(c) \leq k_n$. As n grows, c gets smaller and with a little help from the (euclidean) Ring Lemma one can show carr$(\widehat{q}_n')$ nearly fills the annulus $\mathbb{D}\backslash c$. Thus for sufficiently large n we have

$$\log(1/k_n) \leq 2\text{Mod}(\text{carr}(\widehat{q}_n')).$$

The Ring Lemma and Lemma 3.2 above imply

$$\text{Mod}(\text{carr}(\widehat{q}_n')) \leq \kappa\text{Mod}(\text{carr}(q_n')).$$

Under stereographic projection to $\mathbb{S}^2$, this latter modulus does not change; the image of $\mathrm{carr}(q'_n)$ is a subset of A_n, so finally,

$$\mathrm{Mod}(\mathrm{carr}(q'_n)) \leq \mathrm{Mod}(A_n).$$

Set $M_n = \frac{2}{\kappa}\log(1/k_n)$. This depends only on d, $M_n \to \infty$ as $n \to \infty$, and $M_n \leq \mathrm{Mod}(A_n)$, as desired. With this, we are done with the spherical case.

The positive genus cases are minor variations. In genus 1, the packing p_n may be assumed, with an appropriate lift under the covering map, to lie in $\mathbb{C}$ with $c_{v,n}$ at the origin and lying (by our diameter normalization) within $\mathbb{D}$. The argument of the Length-Area Lemma directly implies that $\mathrm{radius}(c_{v,n})$ goes to zero. When genus is greater than one, p_n lifts to $\mathbb{D}$ and we can put $c_{v,n}$ at the origin. Since p'_n separates $c_{v,n}$ from the unit circle, the euclidean radius of $c_{v,n}$ goes to zero as before; since it is centered at the origin, the same applies to its hyperbolic radius. The bounds only depend on d, so we are done. □

Ever finer control of the geometry emerges under refinement, as we will see in the next section when we apply Rodin and Sullivan's Hexagonal Packing Lemma.

4. Uniformizing Dessins

In this, the central theoretical section of the paper, we connect the classical and discrete Belyĭ pairs. Our work will apply to general triangulations. In the classical setting we introduce the notion of "reflective surfaces" and their refinement by "conformal subdivision". We then show that it is a small step from a refined classical structure to a refined circle packing structure.

4.1. Reflective Structures and Conformal Subdivisions.

The "equilateral" dessin surfaces are examples of what we will refer to as **reflective triangulations**. We work only with triangulations in this paper, but since similiar ideas have been used recently in other settings, we offer a more general definition.

Definition. *A regular cell decomposition $\mathcal{C}$ of a Riemann surface R is **reflective** if, for every edge e of $\mathcal{C}$ in the boundary of two closed faces (2-cells) $f_\pm$, there exists a **conformal reflection** of $f_+ \cup f_-$ across e; explicitly, there exists an idempotent homeomorphism r_e that is anticonformal on $\mathrm{int}(f_+ \cup f_-)$, $r_e(f_\pm) = f_\mp$, the restriction of r_e to e is the identity on e, and r_e exchanges the vertices of $f_\pm$ that do not lie on the edge e. In particular, all cells have the same number of vertices. We say that $\mathcal{C}$ endows R with a **reflective structure**.*

In general, the decomposition of a topological surface S into topological n-gons implies existence of a unique conformal structure in which the decomposition is reflective and the cells are conformally regular n-gons, as in § 2.2. In [6], the plane was endowed with a reflective pentagulation, a refective structure based on pentagonal cells, and work on cubulated manifolds suggests uses for reflective squarings.

Remark. The conformal reflection r_e across the edge e is not globally defined and, indeed, generically will not extend anticonformally beyond its domain of definition $f_+ \cup f_-$. Even in a covering surface, the reflection does not necessarily extend, as is required, e.g., in Wolfart's "mirror-invariant" triangulations in [36]. Though r_e is necessarily angle-preserving at the vertices of $f_\pm$ forming the endpoints of e, it generally will not preserve angles at the remaining vertices of f_+ and f_-. Notice that if v is a vertex of $\mathcal{C}$ of degree d, then the angle between consecutive edges of $\mathcal{C}$ incident at v as determined by the complex structure on R is precisely $\frac{2\pi}{d}$.

Example. Let (S, D) be a dessin with classical Belyĭ map $B_D : S_D \longrightarrow \mathbb{S}^2$. Recall our notation that $S_D = S_\mathcal{T}$, where $\mathcal{T} = \mathcal{T}(D)$ is the canonical triangulation for D. Then $\mathcal{T}$ is a reflective triangulation of S_D: indeed, for any edge e, let B_e be the restriction of B_D to $\mathrm{int}(f_+ \cup f_-)$, where $f_\pm$ are the faces of $\mathcal{T}$ containing e. Then r_e is the continuous extension to $f_+ \cup f_-$ of $B_e^{-1} \circ c \circ B_e$, where c denotes complex conjugation.

Proposition 4.1. *Let $\mathcal{C}$ and $\mathcal{C}'$ be combinatorially isomorphic, reflective cell decompositions of the respective Riemann surfaces R and R'. Then any (orientation-preserving) combinatorial isomorphism of $\mathcal{C}$ with $\mathcal{C}'$ may be realized as a conformal isomorphism of R with R' that takes $\mathcal{C}$ to $\mathcal{C}'$.*

The elementary proof, based on the Schwarz Reflection Principle and removability of isolated singularities, is left to the reader. We state a useful corollary:

Corollary 4.2. *Let $\mathcal{T}$ be a reflective triangulation of the Riemann surface R. Then $R_\mathcal{T}$, the Riemann surface determined by an equilateral metric structured on $\mathcal{T}$, is conformally equivalent to R.*

A triangulation $\mathcal{T}$ of an oriented topological surface not only imposes a conformal structure on the surface, but simultaneously realizes itself as a reflective triangulation *in situ* on the resulting Riemann surface. In our method of uniformizing equilateral surfaces we rely crucially on the fact that $\mathcal{T}$ admits arbitrarily fine subdivisions, what we call *refinements*, which themselves form reflective triangulations of this very same Riemann surface.

A **subdivision** of the triangulation $\mathcal{T}$ of the topological surface S is a triangulation $\mathcal{T}'$ of S such that each cell (vertex, edge, or triangle) of $\mathcal{T}'$ is contained in some cell of $\mathcal{T}$. We are interested in subdivisions of a very special type.

Definition. *If $\mathcal{T}'$ subdivides the triangulation $\mathcal{T}$ of the oriented topological surface S, then $\mathcal{T}'$ is a **conformal subdivision** of $\mathcal{T}$ if there is a subdivision of the reflective triangulation $\mathcal{T}$ of the Riemann surface $S_\mathcal{T}$ that is itself reflective in $S_\mathcal{T}$ and combinatorially isomorphic to $\mathcal{T}'$.*

Lemma 4.3. *If $\mathcal{T}'$ is a conformal subdivision of $\mathcal{T}$, then the associated equilateral surfaces $S_\mathcal{T}$ and $S_{\mathcal{T}'}$ are conformally equivalent. Further, if $\mathcal{T}'$ and $\mathcal{T}$ are realized simultaneously as reflective triangulations of this Riemann surface with $\mathcal{T}'$ subdividing $\mathcal{T}$, and if e is an edge of $\mathcal{T}'$ contained in the edge E of $\mathcal{T}$, then the conformal reflection*

r_e is the restriction of the conformal reflection r_E to the two faces of $\mathcal{T}'$ contiguous along e.

The first assertion of the lemma is important in uniformization, since it will allow us to replace the Riemann surface $S_{\mathcal{T}}$ by $S_{\mathcal{T}'}$, realized as the equilateral surface $|\mathcal{T}'|_{eq}$. However, "conformality" involves an equally important but separate issue: $\mathcal{T}'$ and $\mathcal{T}$ must be realizable simultaneously as reflective triangulations in that common Riemann surface, with $\mathcal{T}'$ subdividing $\mathcal{T}$ *in situ*. As a cautionary example to keep in mind, every triangulation $\mathcal{T}$ of a topological 2-sphere induces the same conformal structure, namely, that of the Riemann sphere $\mathbb{S}^2$. However, for a generic subdivision $\mathcal{T}'$ of $\mathcal{T}$, the *in situ* triangulations $\mathcal{T}'$ and $\mathcal{T}$ will be incompatible.

Proof of 4.3. Since $\mathcal{T}'$ is a conformal subdivision of $\mathcal{T}$, there is a subdivision of the reflective triangulation $\mathcal{T}$ of the Riemann surface $S_{\mathcal{T}}$ that is itself reflective and combinatorially isomorphic with $\mathcal{T}'$. An application of Proposition 4.1 guarentees that the Riemann surfaces $S_{\mathcal{T}}$ and $S_{\mathcal{T}'}$ are conformally equivalent, and the first assertion of the lemma follows. The second assertion follows from the fact that conformal reflections are uniquely determined in a neighborhood of their fixed point sets by those very fixed point sets. □

We are interested primarily in barycentric subdivision and the hexagonal refinements described earlier. These easily are seen to be conformal subdivisions, but for completeness we prove the next result, which provides many additional examples.

Proposition 4.4. *Let τ be an abstract triangulation of a triangle t that has combinatorial dihedral symmetry. Let $\mathcal{T}'$ be a subdivision of $\mathcal{T}$ such that the restriction of $\mathcal{T}'$ to each face of $\mathcal{T}$ is combinatorially equivalent to τ. Then $\mathcal{T}'$ is a conformal subdivision of $\mathcal{T}$.*

Proof. Denote the vertices of t as u_0, u_1, u_2 and recall that $|\tau|_{eq}$ denotes t equipped with an equilateral metric structured on τ. Identifying t with a euclidean unit equilateral triangle $\triangle$, there is a unique homeomorphism $\lambda\colon |\tau|_{eq} \to \triangle$ which fixes u_0, u_1, u_2 and is conformal on the interior of $|\tau|_{eq}$ (recall that the interior of $|\tau|_{eq}$ inherits a conformal structure compatible with its equilateral metric via charts associated with pairs of contiguous equilateral faces, as in § 2.2). By replacing the abstract triangulation τ of t with the image triangulation $\lambda(\tau)$, we may assume, without loss of generality, that τ is a reflective triangulation of the equilateral triangle $\triangle$ that is invariant under the action of the dihedral isometry group $D_{2\cdot 3}$ of $\triangle$. This means, of course, that each edge e of τ that does not lie in the boundary $\partial\triangle$ determines a conformal reflection r_e across e of its two contiguous faces.

In the Riemann surface $S_{\mathcal{T}}$, realized concretely as the equilateral surface $|\mathcal{T}|_{eq}$, let $\mathcal{T}_\tau$ denote the triangulation formed by isometrically mapping the reflective triangulation τ of $\triangle$ onto each face of $\mathcal{T}$ (each a euclidean unit equilateral triangle). The fact that τ is $D_{2\cdot 3}$-invariant guarantees that this gives a well-defined triangulation. We claim that $\mathcal{T}_\tau$ is a reflective triangulation of $S_{\mathcal{T}}$. Indeed, every edge e of $\mathcal{T}_\tau$ whose interior

lies in the interior of a face of $\mathcal{T}$ admits a conformal reflection r_e of its contiguous faces by construction. Further, if e is an edge of $\mathcal{T}_\tau$ contained in an edge of $\mathcal{T}$, then the facts that τ is $D_{2\cdot 3}$-invariant and $\mathcal{T}$ itself is reflective in $S_\mathcal{T}$ imply the existence of a conformal reflection r_e. In fact, if the edge e of $\mathcal{T}_\tau$ is contained in the edge E of $\mathcal{T}$, then, because of the dihedral symmetry across the altitudes of the equilateral triangles, we have $r_e = r_E|(f_+ \cup f_-)$, where $f_\pm$ are the faces of $\mathcal{T}_\tau$ contiguous along e. Thus $\mathcal{T}_\tau$ is a reflective triangulation of $S_\mathcal{T}$ that subdivides $\mathcal{T}$ and, hence, $\mathcal{T}'$, which is combinatorially equivalent to $\mathcal{T}_\tau$, is a conformal subdivision of $\mathcal{T}$. □

Definition. *If τ and $\mathcal{T}$ are as in the proposition, $\tau\mathcal{T}$ denotes a subdivision (or refinement) obtained by subdividing each face of $\mathcal{T}$ according to the combinatorics of τ.*

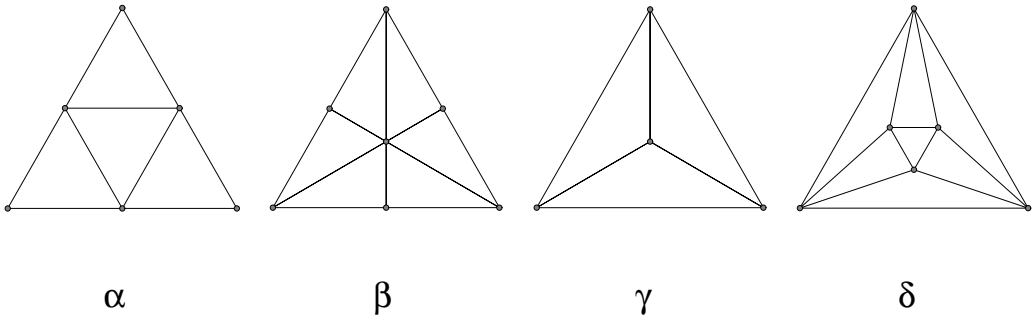

FIGURE 5. Conformal subdivision rules

Figure 5 illustrates four $D_{2\cdot 3}$-invariant triangulations of $\triangle$, denoted α, β, γ, and δ. The first three are conformally correct as shown, since the reflective edges are straight euclidean line segments. The case δ is more generic and its conformally correct form is shown in Figure 6; its reflective edges are some unknown curves, neither euclidean line segments nor euclidean circular arcs. (This image of Figure 6 was obtained by applying essentially the same methods developed below.)

The uniformization algorithm we develop only requires a sequence of refinements whose meshes go to zero, so it will suffice to work with just the hexagonal and barycentric rules, α and β, respectively. We remind the reader of a trait of *hex* refinement that is of crucial importance; namely, *hex* refinement does not raise degree at the original vertices, whereas the others in Figure 5 either double or triple those degrees. We therefore rely on refinement sequences of the form $\{\alpha^n\beta\mathcal{T}\}$, signifying n successive *hex* refinements of an initial barycentric subdivsion of $\mathcal{T}$. The reader will recognize these refinements from Section 3. The notation and terminology of refinements apply equally well, of course, to simplicial complexes which triangulate surfaces.

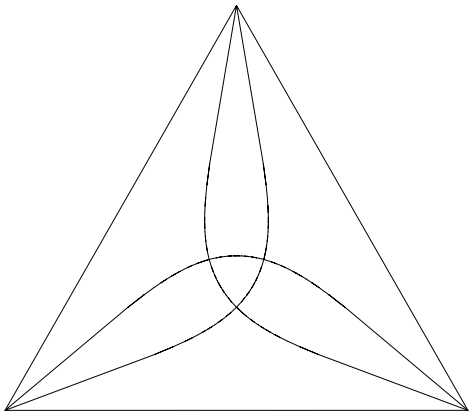

FIGURE 6. The reflective subdivision $\lambda(\delta)$

4.2. **Uniformizing Equilateral Surfaces.** This section establishes the theoretical tools for uniformizing equilateral surfaces, in particular, dessin surfaces. We use many standard results regarding Riemann surfaces and quasiconformal mappings; good references are [19, 11, 20].

Let $\mathcal{T}$ be a triangulation of the compact, connected, oriented topological surface S. Our task is to uniformize the reflective surface $S_{\mathcal{T}}$ determined by the equilateral surface $|\mathcal{T}|_{eq}$. For practical reasons we work with the barycentric subdivision $\beta\mathcal{T}$. Since barycentric subdivision is conformal, the equilateral surface $|\beta\mathcal{T}|_{eq}$ is in the same conformal class as $S_{\mathcal{T}}$. By identifying $S_{\mathcal{T}}$ as the equilateral surface $|\beta\mathcal{T}|_{eq}$ and subdividing each unit equilateral face of $|\beta\mathcal{T}|_{eq}$ into equilateral triangles of side length $\varepsilon(n) = \frac{1}{2^n}$ via n successive *hex* refinements, we realize $S_{\mathcal{T}}$ as $|\mathcal{T}_n|_{eq}^{\varepsilon(n)}$, where $\mathcal{T}_0 = \beta\mathcal{T}$ and $\mathcal{T}_{n+1} = \alpha\mathcal{T}_n$ for $n \geq 0$. Thus, $\{\mathcal{T}_n\}$ is a sequence of reflective triangulations of $S_{\mathcal{T}}$ into triangles, equilateral as seen in the piecewise euclidean metric of $|\mathcal{T}_0|_{eq}$, which are refinements of one another *in situ*, and whose meshes approach zero in the metric of $|\mathcal{T}_0|_{eq}$ as $n \to \infty$.

Note that, unlike the intrinsic metric, the piecewise euclidean metric on the Riemann surface $S_{\mathcal{T}}$ determined by the triangulation $\mathcal{T}_0$ generally is not conformal. Though it is compatible with the complex structure of $S_{\mathcal{T}}$ in the sense that it provides analytic charts for $S_{\mathcal{T}}$ that cover all but the finitely many vertices of $\mathcal{T}_0$, and it is conformal on the complement of these vertices, nonetheless, it fails to be conformal at the non-six degree vertices of $\mathcal{T}_0$. Indeed, though the measure of every angle in every face of $\mathcal{T}_0$ is $\frac{\pi}{3}$ when measured in the euclidean geometry of the equilateral metric, the measure that the Riemann surface $S_{\mathcal{T}}$ ascribes to a particular angle is $\frac{2\pi}{d}$, where d is the degree in $\mathcal{T}_0$ of the associated vertex.

To aid in the readability of what follows, we continue to use abstract simplicial complexes for the combinatorics on the discrete side of things, as in §3. Thus $\mathcal{K} = \mathcal{K}_0$ is the simplicial 2-complex which is combinatorially isomorphic to $\mathcal{T}_0 = \beta\mathcal{T}$, and for each $n \geq 1$, $\mathcal{K}_n = \alpha^n\mathcal{K}$ is obtained from $\mathcal{K}$ by n successive *hex* refinements and is combinatorially isomorphic to $\mathcal{T}_n$.

We are now in position to link the classical and discrete objects. Fix $n \geq 0$. On the classical side we have the Riemann surface $S_{\mathcal{T}}$ with its reflective triangulation $\mathcal{T}_n$; on the discrete side, the Riemann surface $|\mathcal{K}_n|_{cp}$ determined by the circle packing $P_{\mathcal{K}_n}$. Since $\mathcal{K}_n$ and $\mathcal{T}_n$ have been canonically identified, we may consider a vertex v of $\mathcal{T}_n$ simultaneously as a vertex of $\mathcal{K}_n$. We now define the key homeomorphisms h_n from $S_{\mathcal{T}}$ onto $|\mathcal{K}_n|_{cp}$.

Definition. *Let h_n to be a simplicial homeomorphism*

$$h_n : S_{\mathcal{T}} \longrightarrow |\mathcal{K}_n|_{cp}, n = 0, 1, \cdots$$

from the reflective triangulation $\mathcal{T}_n$ of $S_{\mathcal{T}}$ to the carrier $\mathrm{carr}(P_{\mathcal{K}_n})$ *in $|\mathcal{K}_n|_{cp}$ that takes a vertex v in $\mathcal{T}_n$ to the center z_v of the corresponding circle c_v in $|\mathcal{K}_n|_{cp}$ and then extends via barycentric coordinates to map each equilateral triangle uvw in $\mathcal{T}_n$ homeomorphically onto the geodesic triangle $z_u z_v z_w$ in $|\mathcal{K}_n|_{cp}$.*

(When we face the situation in which $|\mathcal{K}_n|_{cp}$ is the sphere, we will have to impose a normalization on $P_{\mathcal{K}_n}$ to ensure that h_n is unambiguous.)

Our approximation results are nicely formulated in the language of Teichmüller space when S has positive genus. Recall that the Teichmüller space $\mathrm{Teich}(S)$ of the surface S consists of equivalence classes $[g]$ of homeomorphisms g from S onto Riemann surfaces S_g, where the homeomorphisms $g : S \longrightarrow S_g$ and $h : S \longrightarrow S_h$ are equivalent whenever the homeomorphism $h \circ g^{-1}$ is homotopic to a conformal isomorphism of S_g onto S_h. The Teichmüller distance between points $[g]$ and $[h]$ of $\mathrm{Teich}(S)$ is

$$\Lambda([g], [h]) = \tfrac{1}{2} \log \inf \kappa(q),$$

where $\kappa(q)$ is the (global quasiconformal) dilatation of q, and q ranges over all quasiconformal mappings in the homotopy class of $h \circ g^{-1}$. This Teichmüller metric Λ is complete, convex, externally convex, and $\mathrm{Teich}(S)$ with the Λ-metric topology is homeomorphic to a finite-dimensional euclidean space — to $\mathbb{R}^2$ if S is a genus 1 surface, and to $\mathbb{R}^{6m-6}$ if S is a genus $m \geq 2$ surface. These and other properties of the Teichmüller metric may be found in [5, 18, 21, 20, 23, 25].

Now the Riemann surface $S_{\mathcal{T}}$ is exactly the topological surface S with a maximal complex atlas determined by pairs of contiguous faces from the triangulation $\mathcal{T}$ realized as euclidean equilateral triangles. Thus the identity mapping $\iota_S \colon S \to S_{\mathcal{T}}$ determines the point $[\iota_S]$ of $\mathrm{Teich}(S)$. Further, the homeomorphisms h_n, by forgetting the complex structure on $S_{\mathcal{T}}$, are mappings defined on S and so provide points $[h_n]$ of $\mathrm{Teich}(S)$. We will show that the homeomorphisms h_n are quasiconformal maps with uniformly bounded dilatations; even though those dilatations are bounded away from unity, we

have the following result, which shows convergence in moduli of the circle packing surfaces $|\mathcal{K}_n|_{cp}$ to the surface $S_{\mathcal{T}}$. In many arguments to follow there is a finite set V^* of points of $S_{\mathcal{T}}$ which must be treated differently; namely, V^* denotes the set of vertices of $\mathcal{T}_0$ that have degree not equal to six.

Theorem 4.5. *If S has nonzero genus, then in the Teichmüller space* Teich(S)*,*

$$\lim_{n\to\infty}[h_n] = [\iota_S].$$

The pointwise dilatations of the maps h_n are bounded above and converge to unity uniformly on compact subsets of $S_{\mathcal{T}}\backslash V^*$.

Proof. We have seen in the results of §3.4 that circle packings induce geometry in a way that controls distortion in a quasiconformal sense. We use this in conjunction with the fact that the Teichmüller metric Λ is proper, meaning that closed Λ-bounded subsets of Teich(S) are compact. This follows, for instance, from the facts that Λ is complete and convex and Teich(S), being homeomorphic to a euclidean space, is locally compact.

By Lemmas 3.1 and 3.2, the restrictions of the homeomorphism h_n to the interiors of the equilateral faces of $S_{\mathcal{T}}$ are κ-quasiconformal, for some κ depending only on the degree of $\mathcal{T}_0$. By removability of analytic arcs and isolated singularities [19], each homeomorphism $h_n : S_{\mathcal{T}} \longrightarrow |\mathcal{K}_n|_{cp}$ is therefore κ-quasiconformal. It follows that *the sequence $[h_n]$ in* Teich(S) *is contained in the closed Λ-ball of radius $\frac{1}{2}\log\kappa$ about the point $[\iota_S]$.*

(The reader might hope that the global quasiconformal dilatations of the h_n converge to unity as $n \to \infty$; however, this generally is not the case. Examine the angle change under h_n at a vertex $a_n \in \mathcal{T}_n$ adjacent a vertex $v \in V^*$. Let f_n be a face of $\mathcal{T}_n$ with v and a_n as vertices. Since $\mathcal{T}_n$ is reflective and f_n is one of exactly six faces that share the vertex a_n, the angle of f_n at a_n has measure precisely $\frac{\pi}{3}$ in $S_{\mathcal{T}}$, for all $n \geq 1$. On the other hand, the corresponding face f_n' of $\text{carr}(P_{\mathcal{K}_n})$ is asymptotically a euclidean isosceles triangle having angle $\frac{2\pi}{d}$ at v, meaning that its angle at a_n approaches $(d-2)\pi/2d$, where $d = \deg(v, \mathcal{T}_0) = \deg(v, \mathcal{K}_n)$. When $d \neq 6$, this value is not $\frac{\pi}{3}$. Fortunately, such unwanted distortion is restricted to ever-shrinking neighborhoods of the vertices of V^*.)

We shall argue that every convergent subsequence of the sequence $[h_n]$ converges to $[\iota_S]$. This and the fact that Λ is proper then imply that every subsequence of $[h_n]$ has $[\iota_S]$ as a limit point, which in turn implies that the original sequence $[h_n]$ converges to $[\iota_S]$. Let $n(1), n(2), \ldots$ be a strictly increasing sequence of positive integers for which the sequence $[h_{n(i)}]$ converges to the point $[h : S \to S_h]$ of Teich(S). Then there is a sequence of quasiconformal homeomorphisms

$$q_i : |\mathcal{K}_{n(i)}|_{cp} \longrightarrow S_h$$

with q_i homotopic to $h \circ h_{n(i)}^{-1}$ and whose global dilatations $\kappa(q_i)$ converge to unity. We have the following diagram of homeomorphisms, with the upper triangle trivially commuting and the lower triangle commuting up to homotopy.

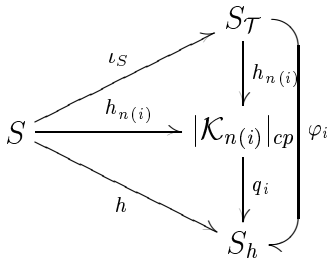

Our aim is to show that the point $[h]$ of Teich(S) is equal to $[\iota_S]$, which will be accomplished by showing that a subsequence of the sequence of quasiconformal homeomorphisms $\varphi_i = q_i \circ h_{n(i)} : S_{\mathcal{T}} \longrightarrow S_h$ converges uniformly to a conformal isomorphism of $S_{\mathcal{T}}$ onto S_h that is homotopic to $h \circ \iota_S^{-1}$. Since the maps $h_{n(i)}$ are κ-quasiconformal and the maps q_i have dilatations $\kappa(q_i)$ converging to unity, all but possibly finitely many of the maps φ_i are 2κ-quasiconformal. Standard arguments in [19] about covergence of sequences of quasiconformal mappings of plane domains applied in the universal covering surfaces of the surfaces $S_{\mathcal{T}}$ and S_h imply that there is a subsequence of the sequence φ_i that converges uniformly to a 2κ-quasiconformal homeomorphism $\varphi : S_{\mathcal{T}} \longrightarrow S_h$. We frame this fact as a separate lemma, which appears, along with its proof, at the end of this proof. Since each map φ_i is homotopic to the fixed map $h \circ \iota_S^{-1}$, it follows that the limit mapping φ is homotopic to $h \circ \iota_S^{-1}$. Modulo the verification of the lemma, our proof that $[h]$ is equal to $[\iota_S]$ is complete once we show that this limit quasiconformal homeomorphism φ is in fact conformal.

Let E be any compact subset of $S_{\mathcal{T}}$ missing the vertices V^*. Our aim is to show that the dilatation of h_n on E goes uniformly to unity as n grows. Let N be an arbitrary positive integer and choose n so large that each point z of E is centered in a simply connected neighborhood U_z formed by $2N$ generations of the hexagonal grid within the reflective triangulation $\mathcal{T}_n$ and missing V^*.

The set U_z is conformally equivalent to the carrier of $2N$ generations of a *regular* hexagonal circle packing, as illustrated in Figure 7(a) for $N = 4$. (In fact, in the equilateral structure $|\beta\mathcal{T}|_{eq}$ of $S_{\mathcal{T}}$, U_z and this carrier are isometric if the circles are given radius $\frac{1}{2^{n+1}}$.) Write $p_{z,n}$ for the circle packing within $P_{\mathcal{K}_n}$ corresponding to U_z.

Let us suppose first that S has genus one. Lift $p_{z,n}$ under the covering map of $|\mathcal{K}_n|_{cp}$ to a circle packing $q_{z,n}$ in $\mathbb{C}$. The restriction of h_n to U_z, with image lifted to $\mathbb{C}$, is precisely the circle packing map from $2N$ generations of a *regular* hexagonal circle packing to $q_{z,n}$, as suggested in Figure 7. By Rodin and Sullivan's Hexagonal Packing Lemma, [28], the maximum pointwise dilatation of h_n in a neighborhood of

z is bounded by a quantity depending only on N which goes to unity as $N \to \infty$. Therefore, the maximum of the pointwise dilatations of the restriction of h_n to E converges to unity, as desired.

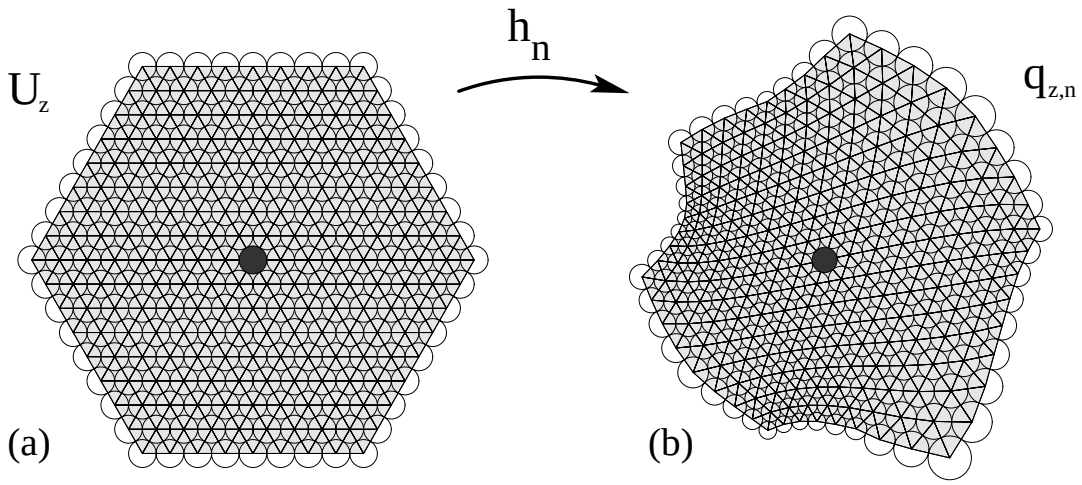

FIGURE 7. h_n restricted to $2N$ hexagonal generations

If S has genus greater than one, our lifted packings $q_{z,n}$ lie in $\mathbb{D}$. However, euclidean geometry is the small scale limit of hyperbolic geometry. By Lemma 3.4, the hyperbolic radii of the circles of $q_{z,n}$ are going uniformly to zero as n grows, so the arguments of the previous paragraph still apply and, again, the pointwise dilatations of the restriction of h_n to E converges to unity.

We have now verified the second part of the theorem. With this it is easy to see that any limit mapping φ of a subsequence of the maps φ_i is conformal. Indeed, since the maximum dilatations $\kappa(q_i)$ converge to unity, the pointwise dilatations of the maps $\varphi_i = q_i \circ h_{n(i)}$ converge to unity uniformly on compact subsets of $S_\mathcal{T} \backslash V^*$. By restricting to simply connected compact subsets of $S_\mathcal{T} \backslash V^*$ and working in the universal covering surface of S_h, we may invoke [19, Theorem II.5.3] to conclude that the restriction of the limit mapping φ to any such compact subset is $(1+\epsilon)$-quasiconformal for every $\epsilon > 0$. It follows that φ is conformal on $S_\mathcal{T} \backslash V^*$ and, by removability of isolated singularities, we conclude that φ is a conformal homeomorphism. This completes the proof of Theorem 4.5, modulo verification of the next lemma. □

Lemma 4.6. *Suppose R and R' are compact, positive genus Riemann surfaces and φ_i is a sequence of κ-quasiconformal homeomorphisms of R onto R'. Then there is a subsequence of the φ_i's that converges uniformly on R to a κ-quasiconformal homeomorphism of R onto R'.*

Proof. Let

$$\pi : \mathcal{D} \longrightarrow R \qquad \text{and} \qquad \pi' : \mathcal{D} \longrightarrow R'$$

be the universal covering projections, where $\mathcal{D}$ denotes appropriately either $\mathbb{C}$ with its usual metric or $\mathbb{D}$ with the Poincaré metric. The groups , and , $'$ of covering transformations of the respective coverings π and π' are groups of Möbius transformations acting properly discontinuously and by isometries on $\mathcal{D}$. Let $\mathcal{F}'$ be the Dirichlet region for , $'$ centered at the origin and, for each i, let z_i be an element of $\mathcal{F}'$ for which $\pi'(z_i) = \varphi_i(\pi(0))$. Let $\Phi_i : \mathcal{D} \longrightarrow \mathcal{D}$ be the lift of the map $\varphi_i \circ \pi$ that sends 0 to z_i, which satisfies $\pi' \circ \Phi_i = \varphi_i \circ \pi$.

$$\begin{array}{ccc} \mathcal{D} & \xrightarrow{\Phi_i} & \mathcal{D} \\ {\scriptstyle\pi}\downarrow & & \downarrow{\scriptstyle\pi'} \\ R & \xrightarrow[\varphi_i]{} & R' \end{array}$$

Since the φ_i's are κ-quasiconformal, so too are their lifts Φ_i, to which we may then apply the convergence theorems of [19, §II.5]. Our claim is that these convergence results imply the existence of a κ-quasiconformal mapping $\Phi : \mathcal{D} \longrightarrow \mathcal{D}$ that is the limit of a subsequence of the Φ_i's whose convergence is uniform on compact subsets of $\mathcal{D}$. It is a straightforward exercise using the discontinuity of the actions of , and , $'$ on $\mathcal{D}$ to show that any such limit mapping Φ takes fibers of π to fibers of π' and therefore induces a κ-quasiconformal homeomorphism $\varphi = \pi' \circ \Phi \circ \pi^{-1}$ that is the limit mapping of a subsequence of the φ_i's. Moreover, the convergence of the subsequence of the φ_i's to φ is uniform since the convergence of the subsequence of the Φ_i's to Φ is uniform on compact subsets of $\mathcal{D}$, in particular, uniform on a compact fundamental domain for , . The verification of the claimed existence of Φ and its nondegeneracy involves looking separately at two cases, genus one and genus greater than one.

In the genus one, or parabolic, case, $\mathcal{D} = \mathbb{C}$. Letting $D = \mathbb{C} - \{0\}$, the restriction of Φ_i to D omits the two values z_i and ∞ of the extended plane $\widehat{\mathbb{C}}$. Their spherical separation is bounded below because $z_i \in \mathcal{F}'$ and $\mathcal{F}'$ is bounded in $\mathbb{C}$, and so the family $\{\Phi_i|D\}$ of κ-quasiconformal mappings of D into $\widehat{\mathbb{C}}$ is normal. It follows that a subsequence of these mappings converges uniformly (in the spherical metric) on compact subsets of D to a limit mapping $\Phi : D \longrightarrow \widehat{\mathbb{C}}$. Since the points $z_i = \Phi_i(0)$ are all in the compact set F', by passing to a further subsequence if necessary, we may assume that the points z_i converge to a point $w \in \mathcal{F}'$, allowing us to define $\Phi(0) = w$. Thus a subsequence of the maps Φ_i converges to $\Phi : \mathbb{C} \to \widehat{\mathbb{C}}$. There are exactly three possibilities: the limit function Φ is either a constant mapping, a mapping of $\mathbb{C}$ onto two points of $\widehat{\mathbb{C}}$, or a κ-quasiconformal mapping of $\mathbb{C}$. We leave it to the reader to eliminate the first two possibilities by using the fact that the maps Φ_i cover the maps φ_i.

For higher genus, the hyperbolic case, $\mathcal{D} = \mathbb{D}$, we get normality of the family $\{\Phi_i\}$ for free, and therefore some subsequence converges uniformly on compact subsets of $\mathbb{D}$ to a mapping Φ. The limit function Φ is either a constant mapping of $\mathbb{D}$ onto a boundary point of $\mathbb{D}$ or a κ-quasiconformal mapping of $\mathbb{D}$ onto itself. Since the points $\Phi_i(0)$ all lie in the compact set $\mathcal{F}'$, the first possibility is precluded and we are done. □

The convergence in Theorem 4.5 can be stated in a more concrete form if we apply the reasoning just used with this lemma. As we did there, let $\mathcal{D}$ denote the universal covering surface of $S_{\mathcal{T}}$ ($\mathbb{D}$ or $\mathbb{C}$), $\pi : \mathcal{D} \longrightarrow S_{\mathcal{T}}$ the (analytic) universal covering projection, and , $\subset \mathrm{Aut}(\mathcal{D})$ the covering group. The triangulation $\mathcal{T}$ in $S_{\mathcal{T}}$ lifts under π to an infinite triangulation $\mathcal{T}^\infty$ of $\mathcal{D}$ invariant under , . Within $\mathcal{T}^\infty$ one can identify a finite union $\mathcal{F}$ of triangles which forms a simply connected fundamental domain of the covering. This concrete setting requires normalization: identify vertices $\nu_0, \nu_1 \in \mathcal{F}$ so that $u_0 = \pi(\nu_0)$ and $u_1 = \pi(\nu_1)$ are neighboring vertices of $\mathcal{T}$; we will always apply a conformal automorphism to $\mathcal{D}$ so that ν_0 is located at the origin and ν_1 is on the positive real axis in $\mathcal{D}$. The conformal data pertaining to $S_{\mathcal{T}}$ is encoded in $\mathcal{F}$, and in particular, in the locations of the boundary vertices of $\mathcal{F}$. From these (and knowledge of the side-pairings of $\mathcal{F}$) one can generate the covering group, which is (up to conjugation) uniquely associated with the point $[\iota_S]$ of $\mathrm{Teich}(S)$.

We can carry out the analogous process for each Riemann surface $|\mathcal{K}_n|_{cp}$. For $n \geq 0$, its universal covering surface is again $\mathcal{D}$; we write $\pi_n : \mathcal{D} \longrightarrow |\mathcal{K}_n|_{cp}$ for the covering projection, , $_n$ for the covering group. We may identify a fundamental domain in $\mathcal{D}$, call it $\mathcal{F}_n$, which corresponds combinatorially (under our usual identification of $\mathcal{K}_n$ with $\mathcal{T}$) to $\mathcal{F}$; designated vertices $\nu_0^{(n)}, \nu_1^{(n)} \in \mathcal{F}_n$ lie over u_0, u_1, respectively, and we impose the same normalization as before. Note that $\mathcal{F}_n$ is combinatorially just the refinement $\alpha^n\beta\mathcal{F}$. The ordered list of vertices about $\partial\mathcal{F}$ occur (in order) among the vertices of $\partial\mathcal{F}_n$, each μ of $\partial\mathcal{F}$ occurs as a vertex $\mu_n \in \partial\mathcal{F}_n$ so that $v = \pi(\mu) \in \mathcal{T}$ corresponds to $v = \pi_n(\mu_n) \in \mathcal{K}_n$.

Lifting the maps defined earlier from the surface level up to $\mathcal{D}$, one obtains maps H_n defined by

$$H_n = \pi_n^{-1} \circ h_n \circ \pi, \qquad H_n(0) = 0, \qquad H_n(\nu_1) > 0.$$

Each H_n is a homeomorphism of $\mathcal{D}$ with $H_n(\mathcal{F}) = \mathcal{F}_n$. Standard arguments yield the following corollary to Theorem 4.5.

Corollary 4.7. *The homeomorphisms $H_n : \mathcal{D} \longrightarrow \mathcal{D}$ converge uniformly on compact subsets of $\mathcal{D}$ to the identify function. In particular, for each boundary vertex μ of $\mathcal{F}$, the sequence $\{\mu_n\}$ of corresponding boundary vertices of $\mathcal{F}_n$ satisfies*

$$\lim_{n\to\infty} \mu_n = \mu.$$

Likewise, for the covering groups,

$$\lim_{n\to\infty} \, , \, _n = \, , \, ,$$

where convergence is in the usual topology of $Aut(\mathcal{D})$.

In the case that our equilateral surface is associated with a dessin (S, D), this corollary tells us that within the universal covering surface one can essentially see the convergence of the discrete dessin surfaces $s_D^{(n)}$ to the classical dessin surface S_D. The reader will find several examples in the Menagerie.

When S is a genus zero surface, Teich(S) is a singleton and the limit result of Theorem 4.5 is automatic, and uninteresting. Here $S_{\mathcal{T}} = \mathbb{S}^2$, and the maps $h_n : \mathbb{S}^2 \longrightarrow \mathbb{S}^2$ are not defined in a conformally invariant fashion. However, our next result shows that appropriate normalizations of the h_n will again be quasiconformal, with dilatations converging to unity off V^*; in other words, we still have rigidity waiting to be exploited.

For purposes of normalization, fix distinct vertices v_0, v_1, v_∞ of the triangulation $\mathcal{T}$. We assume that each packing $P_{\mathcal{K}_n}$ has been adjusted by a conformal automorphism of $\mathbb{S}^2$ to put v_i at i; thus $h_n(v_i) = i$, for $i = 0, 1, \infty$. (When $\mathcal{T} = \mathcal{T}(D)$, we have already designated such vertices.)

Theorem 4.8. *If S has genus zero, then the (normalized) maps $h_n : \mathbb{S}^2 \longrightarrow \mathbb{S}^2$ converge uniformly to a conformal automorphism, with the pointwise dilatations of the h_n converging to unity uniformly on compact subsets of $\mathbb{S}^2 \backslash V^*$.*

Proof of theorem. By Lemmas 3.4 and 3.1, for N sufficiently large, each map h_n is κ-quasiconformal. [19, Theorem II.5.1] immediately implies that $\{h_n\}$ forms a normal family of maps, and [19, Theorem II.5.3] implies that every limit function of this family is κ-quasiconformal. Lemma 3.4 implies that the local geometry of the packings $P_{\mathcal{K}_n}$ is infinitesimally euclidean. Therefore, in arguments similar to those in the proof of Theorem 4.5, the Hexagonal Packing Lemma implies the uniform convergence of the dilatations to unity on compact subsets missing V^*, and this in turn implies that every limit function of the family $\{h_n\}$ is conformal. If f and g are two such limit functions, then the composition $g \circ f^{-1}$ is a conformal mapping of the Riemann sphere that fixes the three points $0, 1$, and ∞, hence, $f = g$. This and the normality of the family imply that the maps h_n converge uniformly to a conformal automorphism. □

4.3. **Convergence of the Belyĭ Maps.** Given a dessin (S, D) and applying Theorem 4.5 to the triangulation $\mathcal{T}(D)$, we conclude that the associated discrete dessin surfaces $s_D^{(n)}$ converge to the classical dessin surface S_D in Teichmüller space. We now establish the convergence, in an appropriate sense, of the discrete Belyĭ maps $b_D^{(n)}$ to the classical Belyĭ map B_D.

First, one should note the **discrete reflective structure** within $|\mathcal{K}_n|_{cp}$ that parallels the classical reflective structure of $S_{\mathcal{T}}$. This analogue is visually apparent in packing

illustrations, such as Figure 2 and Figure 3 or later illustrations in the Menagerie. For contiguous shaded and unshaded faces, the reflection across the shared edge should simply interchange the carriers of the packings of the two faces; under refinement we would expect this map to become increasingly more anticonformal. We already have in the homeomorphisms h_n the appropriate machinery. The image $h_n(\mathcal{T})$ of the reflective triangulation $\mathcal{T}$ of $S_{\mathcal{T}}$ provides a triangulation of $|\mathcal{K}_n|_{cp}$. Given an edge $e \in \mathcal{T}$ and contiguous faces $f_\pm$, recall the edge reflection r_e in $S_{\mathcal{T}}$; the discrete edge reflection is define by

$$r_e^{(n)} = h_n \circ r_e \circ h_n^{-1}.$$

This is an idempotent quasiconformal homeomorphism interchanging $h_n(f_\pm)$ precisely as suggested visually.

Theorem 4.5 (and Theorem 4.8 in the genus 0 case) implies that $r_e^{(n)}$ is nearly anticonformal away from V^*. To be more precise, recall that our definition of the maps h_n begins with the surface $S_{\mathcal{T}}$ realized concretely as the equilateral surface $|\beta\mathcal{T}|_{eq}$, so the face f_+ is realized in $|\beta\mathcal{T}|_{eq}$ as the union of six equilateral triangles forming a flat euclidean hexagon. The homeomorphism h_n is then obtained only after n iterations of *hex* refinement. Let $e^{(n)}$ and $f_\pm^{(n)}$ denote the images $h_n(\alpha^n\beta e)$ and $h_n(\alpha^n\beta f_\pm)$ in the circle packing surface $|\mathcal{K}_n|_{cp}$. Let U be a (small) neighborhood of the vertices of $V^* \cap \alpha^n\beta(f_+ \cup f_-)$. There are at most nine such vertices, up to four forming the original vertices of the two faces $f_\pm$ and five (4-degree vertices) forming the barycenters of the original edges of these two faces. Let U_n denote the image $h_n(U)$ and let κ_n denote the maximum dilatation of $r_e^{(n)}$ taken over the set $(f_+^{(n)} \cup f_-^{(n)})\backslash U_n$. Theorems 4.5 and 4.8 imply the following result.

Proposition 4.9. *For any edge e of $\mathcal{T}$ and neighborhood U as above, the corresponding sequence κ_n of dilatations converges to unity.*

It is important to observe from this result that when numerically uniformizing reflective surfaces, one obtains not only approximate fundamental regions, as in Corollary 4.7, but also a triangulation of that fundamental region which has the combinatorics of $\mathcal{T}$ and approximates the conformally correct reflective triangulation in the surface $S_{\mathcal{T}}$. In the zero genus case, the numerical uniformization gives a triangulation of the Riemann sphere into nearly reflective triangles whose vertices and edges are close to their conformally correct positions. In the case that $\mathcal{T}$ is the canonical triangulation $\mathcal{T}(D)$ of a dessin D, the numerical uniformization provides the approximate locations of points that branch over $0, 1$, and ∞ under a Belyĭ map, as well as the approximate pre-image of the extended real line under that map. The authors know of no other general method for obtaining such approximations.

Recall from Proposition 3.3 that the discrete Belyĭ maps are κ-quasiregular. The next result guarantees that the Belyĭ map B_D may be approximated as closely as desired by these discrete ones.

Theorem 4.10. *Given a dessin (S, D) and the associated discrete Belyĭ maps $b_D^{(n)}$, define the maps*

$$\beta_n = b_D^{(n)} \circ h_n : S_{\mathcal{T}} \longrightarrow \mathbb{S}^2, \quad n \geq 0.$$

Then the sequence $\{\beta_n\}$ converges uniformly on $S_{\mathcal{T}}$ to the Belyĭ map B_D. The pointwise dilatations of the maps β_n converge to unity uniformly on compact subsets of $S_{\mathcal{T}} \backslash V^*$.

Proof. The proof is similar to those of Theorems 4.5 and 4.8. Fix a (+)triangle f of the dessin triangulation $\mathcal{T} = \mathcal{T}(D)$. As in the proof of Threorem 4.8, the Ring Lemma and [19, Theorem II.5.1] imply that the restrictions of the maps β_n to f form a normal family of κ-quasiconformal maps, for some constant $\kappa \geq 1$. By [19, Theorem II.5.5], every limit function of this family must be either a κ-quasiconformal homeomorphism or a mapping onto a single point in the extended real line. We verify in the next paragraph that the former possibility holds for every limit function. Assuming this for the moment, an argument as in the proof of Theorem 4.8, using the fact that any limit function must take the i-vertex of f to the point i, for $i = 0, 1, \infty$, implies that the restrictions of the β_n's to f converge to a conformal map taking the boundary ∂f to the extended real line $\widehat{\mathbb{R}}$. Immediately, this limit function must be the unique conformal mapping of f onto the upper half plane that takes the i-vertex of f to i. This is precisely the restriction of the Belyĭ map B_D to f. The same argument works if f is any $(-)$triangle. It follows that the maps β_n converge uniformly to the Belyĭ map B_D. The dilatation convergence (already used when the argument of Theorem 4.8 was applied) follows as in the proof of Theorem 4.5.

We now verify that any limit function of the normal family of maps described in the previous paragraph takes at least one value in the (open) upper half plane. Recall the abstract simplicial complex $\mathcal{H}$ triangulating the sphere, defined in § 3; let v denote the vertex corresponding to the barycenter of the upper half plane, one of the two faces of $\mathcal{H}$. Recalling that v is then contained in all the *hex* refinements $\alpha^n\mathcal{H}$ of $\mathcal{H}$, let $z(n)$ denote the center of the circle c_v in the circle packing $Q^{(n)}$ for $\mathcal{H}_n = \alpha^n\mathcal{H}$. The definitions of h_n and $b_D^{(n)}$ guarantee that the restriction of each map β_n to the (+)triangle f satisfies $\beta_n(\widehat{z}) = z(n)$, where $\widehat{z}$ is the (unique) conformal barycenter of f. Since the restriction of each map β_n to f is a κ-quasiconformal homeomorphism onto the upper half plane, it suffices to show that the points $z(n)$ are bounded away from the extended real line. In fact, however, the $z(n)$ form a constant sequence: each $z(n)$ is precisely the point $e^{\pi i/3}$, which is the (unique) conformal barycenter of the upper half plane thought of as a triangle with vertices 0,1, and ∞ and sides forming the extended real line. This follows from the fact that the circle packing $Q^{(n)}$ inherits order six dihedral symmetry from that of $\mathcal{H}_n$; this symmetry permutes the circles centered at 0,1, and ∞ and hence fixes the circle corresponding to the barycenter $\widehat{z}$. □

5. A Menagerie of Dessins d'Enfants

For convenience, the Menagerie is organized by genus. As opportunities arise, we point out various pertinent features, many of which will apply in several settings. We will refer back to these examples when we discuss computational issues in Section 6, but at this point we should remark on the two senses in which these examples are "approximations". First, all are subject to the usual round-off and truncation errors of numerical computation and display; second, even were we to have perfect information on a given discrete dessin, that dessin might only approximate its classical companion.

5.1. **Genus 0.** In the case of the sphere, the conformal structure engendered by a dessin is not at issue — the sphere has only one. We have latitude only in the normalization, and we have agreed to the convention that designated i-vertices are placed at i for $i = 0, 1, \infty$. In such a normalized situation, the conformally correct dessin, the location of zeros, ones, and poles, and various other metric information are examples of data of interest.

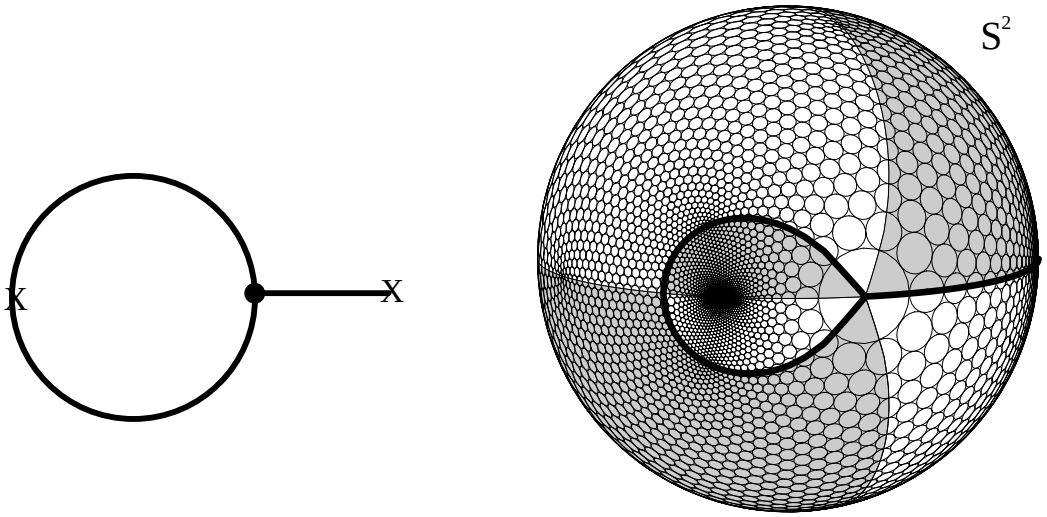

Figure 8. Dessin 1 and its stage-4 packing in $\mathbb{S}^2$

5.1.1. *Example 1.* We begin with the very simple dessin D of Figure 8(a). This is the only example we give which fails to be "clean"; it has a "free" edge ending in a $\times$, so its Belyĭ map will not branch at this 1-vertex. The stage-4 packing $P_D^{(4)}$ is shown in Figure 8(b). As will be standard, we shade appropriate faces and mark the dessin itself with a heavy line.

5.1.2. *Example 2.* We have used a clean dessin only slightly more complicated than the previous example for purposes of illustration earlier in the paper; we denote it Example 2. The dessin and its triangulation are displayed in Figure 1, its stage-3 discrete Belyĭ map in Figure 2, and its coarse discrete Belyĭ map in Figure 3. In Figure 9 we project its stage 3 packing to the plane for comparison to Figure 1.

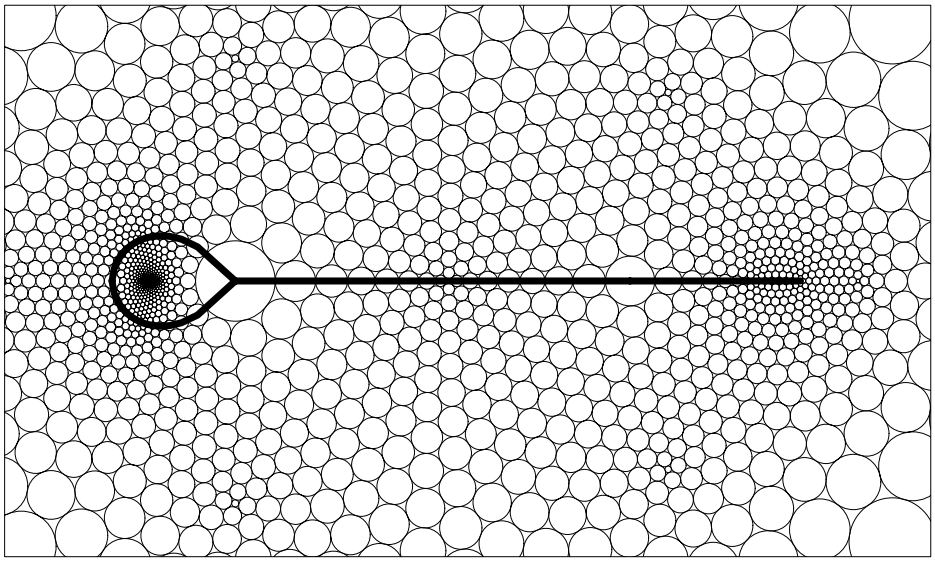

FIGURE 9. Stereographic projection of Dessin 2

5.1.3. *Example 3.* We add further edges to the dessins of Examples 1 and 2 to get Dessin 3 of Figure 10(a). (See §6.1 concerning "dessin moves".) Stereographic projections of the discrete dessin as embedded by the coarse and first four stages of hex refinement are given in Figure 11, illustrating the evolving shape. Detail around the head at stage-4 is shown in Figure 12.

This dessin, due to Gunter Malle (see [16]) has a known and nontrivial orbit. Recall that dessins are associated with number fields. The Galois group of the number field provides an action on dessins, and the Galois orbit of a dessin is the smallest collection of dessins closed under the Galois action. In the case of Example 3, the Galois orbit consists of Dessin 3 and the dessin of Figure 10(b) — in other words, the Galois action switches between the left-arm person and her right-arm companion!

5.1.4. *Example 4.* Trees form the only general class of dessins for which approximation methods have been developed. Dessin 4 is a tree from [29]. The embedded image of Figure 13 is from the stereographic image of $P_D^{(4)}$ and should be compared to the image [29, p. 112]. Using Grobner basis methods, Couveignes and Granboulan can provide extreme accuracy for embedded trees, enough to eventually recover coefficients

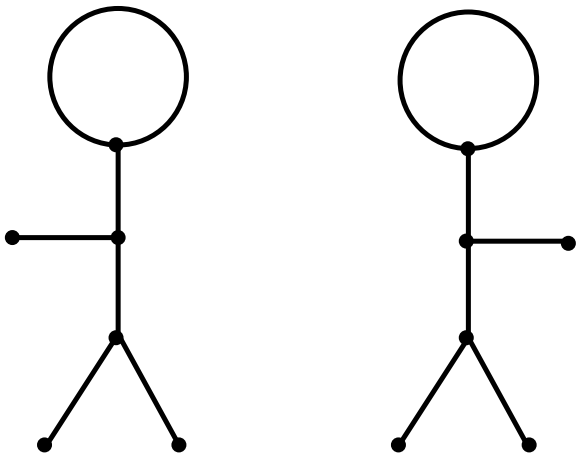

FIGURE 10. Dessin 3: A genus 0 Galois orbit

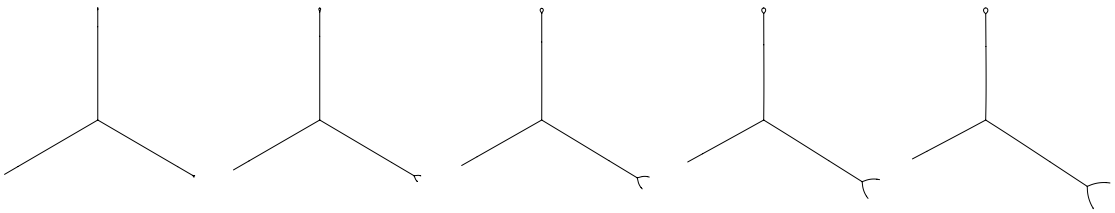

FIGURE 11. Successively finer stages of the right-armed dessin

of defining equations. (The equation for Dessin 4 has integer coefficients of over twenty digits!) This far surpasses the accuracy available *via* circle packing. However, their methods involve certain initial guesses for locations of vertices and the addition of vertices to existing trees. Circle packing might prove very helpful in this process; see especially §6.1.

5.2. **Genus 1.** A dessin has genus 1 if it is drawn on the topological 1-torus $\mathbb{T}$. The torus has the euclidean plane as its universal cover, and $\mathbb{T}$ endowed with a conformal structure is typically identified with a fundamental domain in $\mathbb{C}$. The lift to the plane of any point on the conformal torus forms a doubly periodic lattice, and the ratios of

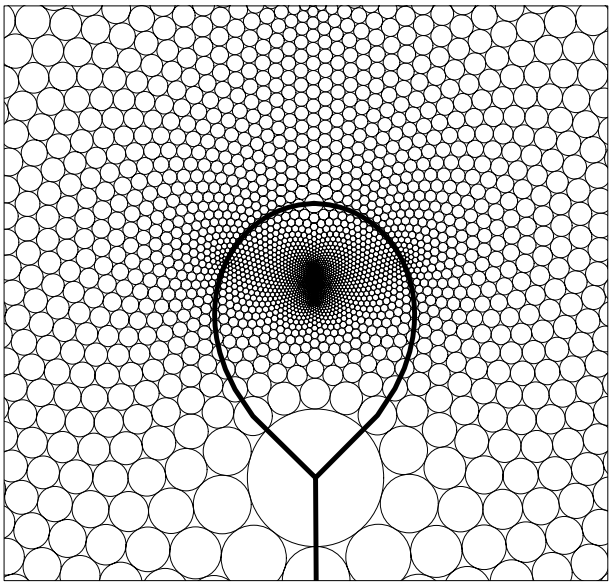

FIGURE 12. Stereographic projection of the head of Dessin 3

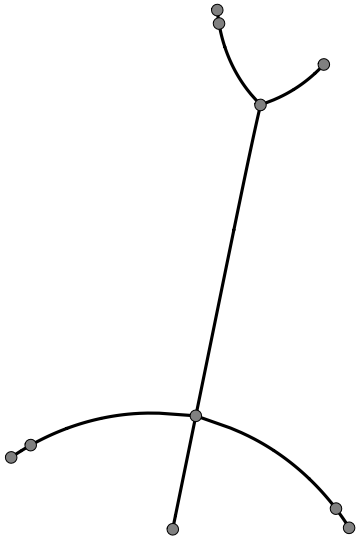

FIGURE 13. A dessin tree

pairs of complex numbers generating that lattice parameterize the conformally distinct marked tori. We will see this played out in its discrete form here.

We concentrate on a dessin introduced by Shabat and Voevodsky [30] and thoroughly analyzed by them and others. In this case the associated number field, the defining

equation, the Galois orbit, and the parameters of the associated tori are known, affording one an opportunity to compare the discrete and classical information.

5.2.1. *Example 5.* Dessin 5 is illustrated in Figure 14(a), where opposite sides of the rectangle are identified in the usual way so that the dessin is seen to lie on $\mathbb{T}$.

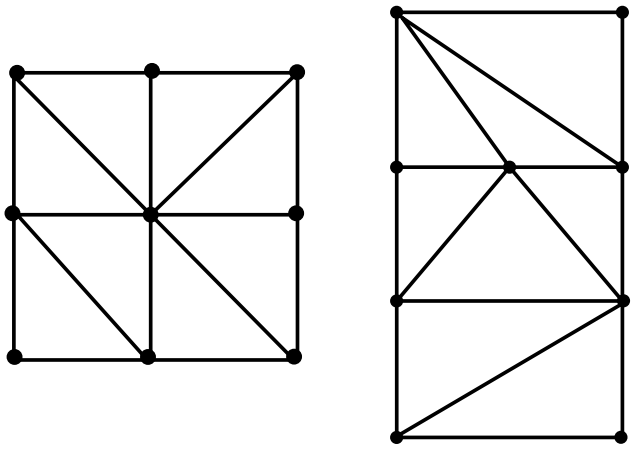

FIGURE 14. Dessins 5 and 6: A genus 1 Galois orbit

From Dessin 5 one obtains the canonical triangulation of $S = \mathbb{T}$ and its barycentric subdivision $\mathcal{K}$. There is a unique conformal torus s_D, the coarse dessin surface, which supports the circle packing $P_{\mathcal{K}}$ for $\mathcal{K}$; in this genus 1 case, the metric is euclidean, hence only defined up to a multiplicative positive constant.

As in the classical setting, one may represent s_D by lifting to the universal covering surface, $\mathbb{C}$. In fact, everything lifts: the triangulation, the complex, the circle packing, the metric, and the dessin. The results for the coarse packing of Dessin 5 are illustrated in Figure 15(a), with a fundamental domain highlighted.

We are in position to estimate the conformal modulus of the discrete torus. The four corners of the fundamental domain in Figure 15(a) correspond to the same point of s_D and define the covering lattice in $\mathbb{C}$. From the packing centers one can read off approximations to a pair of complex numbers which generate the lattice. For convenience we have placed the lower edge of the packing with ends at 0 and 1 in Figure 15(a); the complex number associated with the left side is approximately $\tau \approx 0.249612 + 0.968346i$; we will refer to this information in §6.

Of course we have the option of refining our circle packing for a more accurate approximation of the classical dessin. Using 2 stages of hex refinement and repacking leads to the fundamental domain of Figure 15(b) for $s_D^{(2)}$. Again, the lower corners

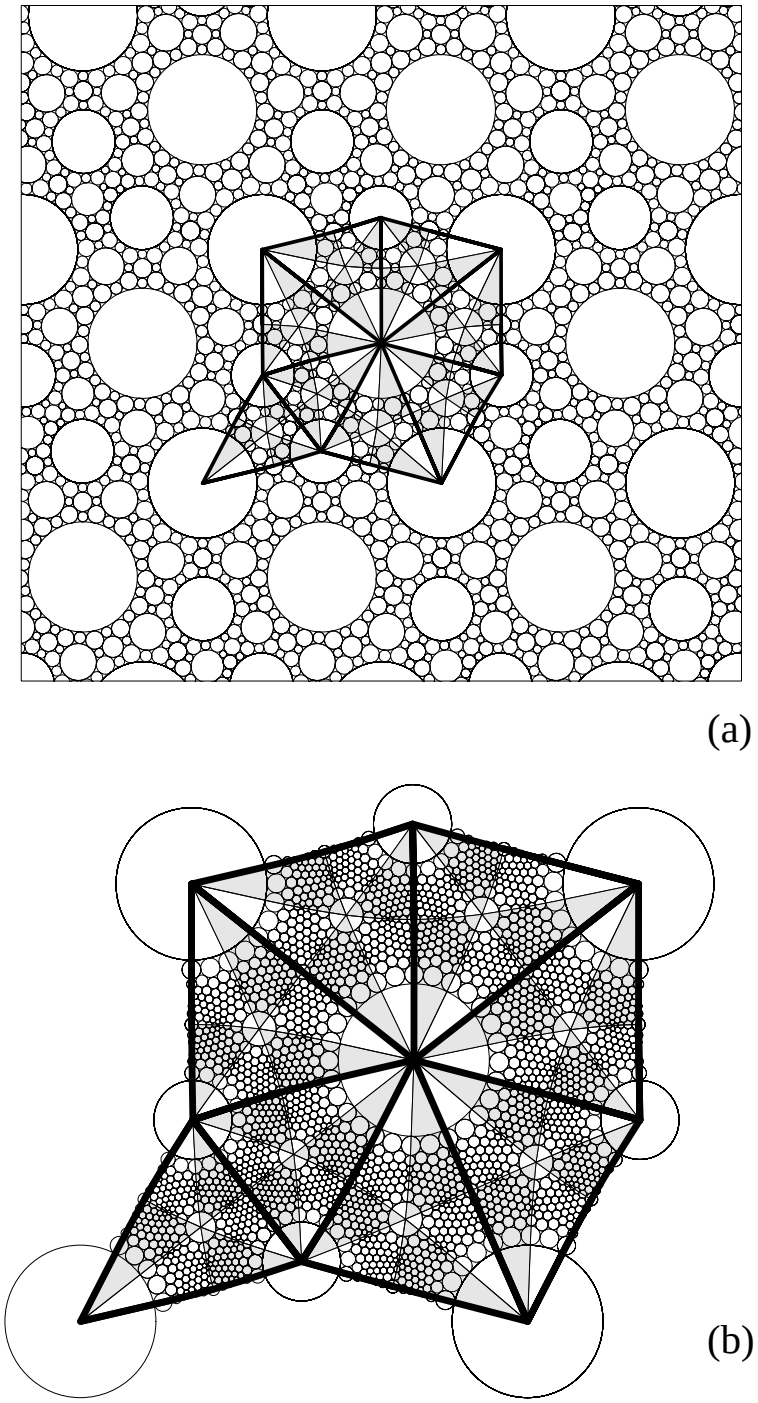

FIGURE 15. Fundamental domains for genus 1 packings

have been placed at 0 and 1, and the complex number for the other side can be read off as approximately $\tau \approx 0.248308 + 0.968683i$.

5.2.2. *Example 6.* The Galois orbit for Dessin 5 contains one other dessin, shown in Figure 14(b). Dessin 6 is laid out using the stage-2 packing $s_D^{(2)}$ in Figure 16. This illustrates the general fact (see [15]) that conjugate dessins share the same numbers of dessin faces, edges, and vertices. (Their circle packings consequently share the same number of circles at each refinement stage.) Dessins 5 and 6 should be compared, both in their schematic and embedded forms, to [2, Fig. 8, p. 209] and [30, p. 215].

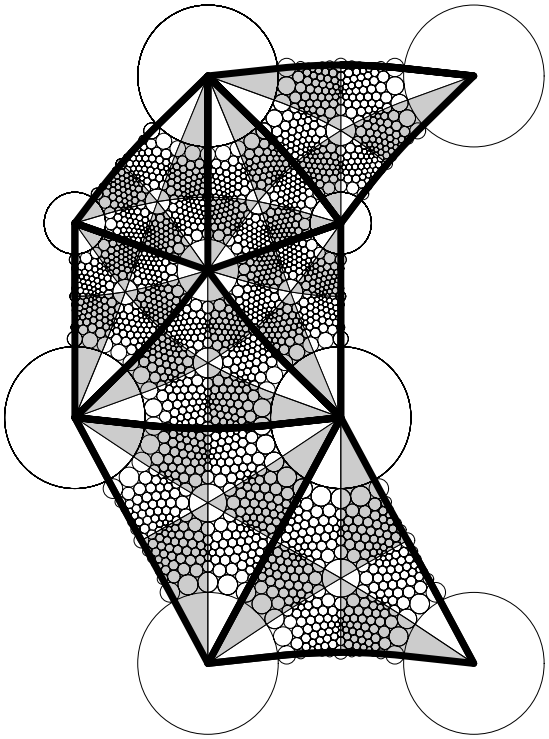

FIGURE 16. The Galois conjugate of Dessin 5

5.3. **Genus 2.** With higher genus we move into the hyperbolic realm. The dessin surfaces are covered now by the hyperbolic plane, which we will represent as the unit disc $\mathbb{D}$ endowed with the Poincarè metric $ds = 2/(1 - |z|^2)|dz|$ of constant curvature -1. In a manner completely analogous to the previous genus 1 setting, one may lift all structures from the surface to a fundamental domain $\mathcal{F}$ of the covering. The covering group , is now a discrete nonabelian group of automorphisms of $\mathbb{D}$. We will illustrate with three examples.

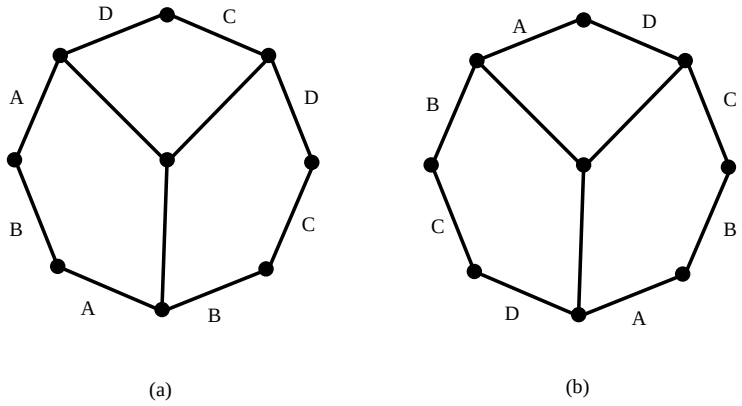

FIGURE 17. Dessins 7 and 8: Two dessins of genus 2

5.3.1. *Example 7.* Dessin 7 is shown in Figure 17(a); it is important to note the identifications of the sides which makes this into a surface of genus 2. When triangulated, Dessin 7 contains 28 faces. The associated coarse circle packing is shown in Figure 18(a) and the stage-3 refinement in Figure 18(b). In each case, a 0-point has been placed at the origin and only fundamental domains $\mathcal{F}_0$ and $\mathcal{F}_3$, respectively, are shown; the numbering of boundary edges for the side-pairings is indicated on the coarse packing. In each case, the action of the covering group $,_n$ generates a tiling of the hyperbolic plane with isometric images of $\mathcal{F}_n$.

A few observations are in order. The eight circles at the cusps on the boundary of $\mathcal{F}_0$ are in fact eight lifts of one circle; in particular, although their radii are euclideanly different because of their distances from the boundary, they share a common hyperbolic radius. The angles at the cusps sum to 2π, and in the fundamental domain for the classical surface would all be precisely $\pi/4$. A cautionary note: the edges between cusps in these figures are approximating analytic arcs; though they may appear to be approximate geodesics, this need not be the case.

This dessin provides an opportunity to illustrate Corollary 4.7. In particular, *the circle packing for a discrete dessin provides numerical estimates of the covering maps of the associated classical dessin surface.* Estimation occurs in two stages which we now discuss. (The same general considerations applied in the euclidean setting of Example 5.)

Step 1: First is the estimation of the covering maps for a discrete dessin surface. In Figure 18(a), let $\{c_1, \cdots, c_8\}$ denote the eight cusp points of $\mathcal{F}_0$. Each side-pairing of $\mathcal{F}_0$ is associated with an element $\gamma \in ,_0$ which carries one ordered pair of these points to another: $\gamma : (c_i, c_j) \mapsto (\gamma(c_i), \gamma(c_j))$. This information alone determines the

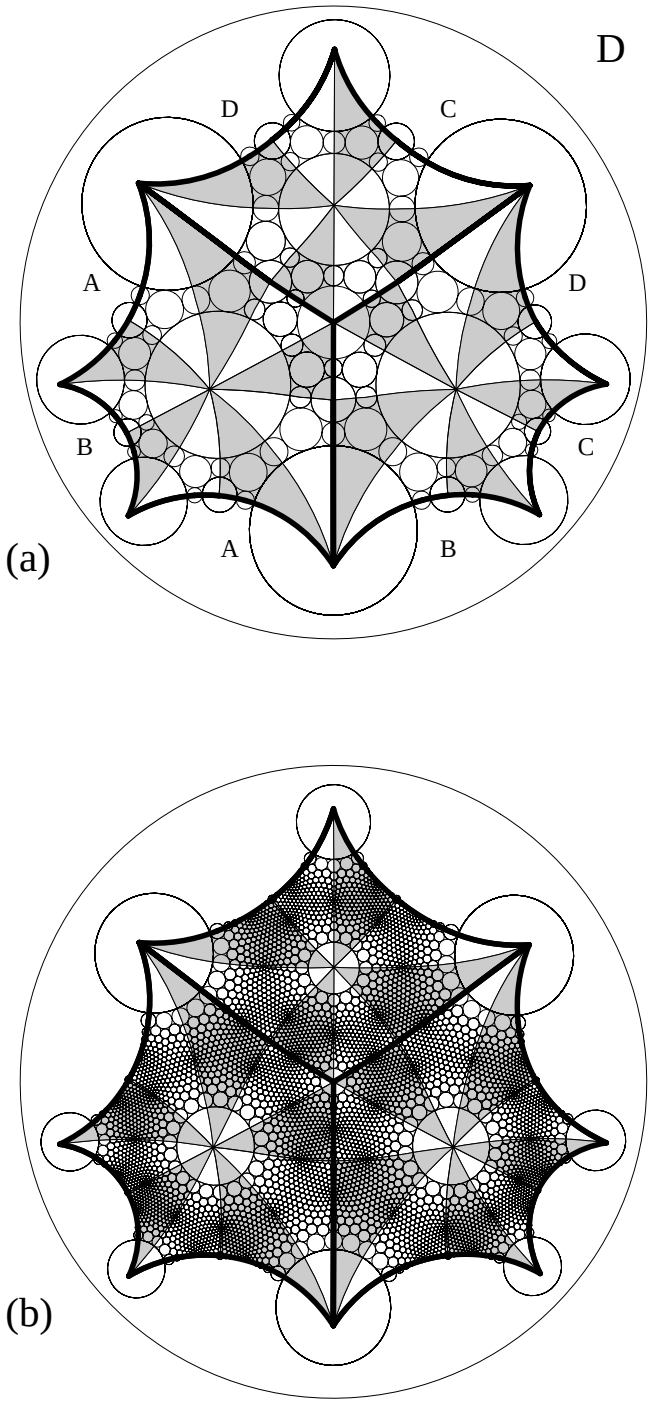

FIGURE 18. Coarse and stage-3 fundamental domains for Dessin 7

automorphism γ. In turn, such side-pairing automorphisms γ generate $,_0$. Therefore, the locations and pairings of the eight points c_j determine $,_0$. In theory, this information is exact, but in practice, of course, the data is subject to roundoff errors in the computation of packing radii, the location of the centers, and the subsequent computation of the automorphisms.

Step 2: The second stage involves the use of successively finer circle packings so that their covering maps converge to the classical covering maps. Figure 18(b) is the stage-3 hex refinement, involving 5374 circles. The computed locations of the eight cusp points give estimates for the associated side-pairing maps. Matrices in $\mathrm{GL}(2,\mathbb{C})$ representing the A, B, C, and D side-pairings (see Figure 18) are given by, respectively,

$$\begin{bmatrix} 0.610254 - 0.705705i & -0.725003 + 0.416873i \\ -0.725003 - 0.416873i & 0.610254 + 0.705705i \end{bmatrix}$$

$$\begin{bmatrix} -0.389727 + 0.416402i & 0.511033 + 0.158976i \\ 0.511033 - 0.158976i & -0.389727 - 0.416402i \end{bmatrix}$$

$$\begin{bmatrix} -0.426400 + 0.422296i & -.0443194 + 0.336691i \\ -.0443194 - 0.336691i & -0.426400 - 0.422296i \end{bmatrix}$$

$$\begin{bmatrix} 0.532299 - 0.413640i & 0.605959 - 0.0348912i \\ 0.605959 + 0.0348912i & 0.532299 + 0.413640i \end{bmatrix}$$

It seems clear that estimates of the type obtained here do not provide perfect information — a precise number field, for example — about the dessin surface. However, they do provide what would normally be considered as fundamental information for one to "know" its conformal structure. The data should be sufficient, for instance, to invoke some of the available programs for working numerically with Riemann surfaces, such as the CARS program of the HCM network on Computational Conformal Geometry and the Symbolic Computation Group at Florida State University.

Example 7 is a favorite of the authors because it was the first hyperbolic example attempted: we were surprised with the speed, beauty, and accuracy of the process. The accuracy still seems remarkable, and we comment on this in the next section.

5.3.2. *Example 8.* Dessin 8, shown in Figure 17(b), differs from the previous example in its side-pairings. The coarse packing is shown in Figure 19(a), and a visual comparison with Figure 18 suggests that these surfaces are conformally very close. Are they the same surface? Is this, in fact, the same dessin?

5.3.3. *Example 9.* Here we show a somewhat more generic genus 2 dessin; the dessin and its faces, as embedded by a stage-2 packing, are laid out in Figure 19(b). One side-pairing has been highlighted to demonstrate that this is clearly not a standard fundamental domain bounded by geodesics.

This dessin was constructed to provide one simple handle and one with richer combinatorics. The resulting asymmetry in their conformal structures is evident. (One "handle" consists of the two cells at the top, the other of the nine lower cells.) This

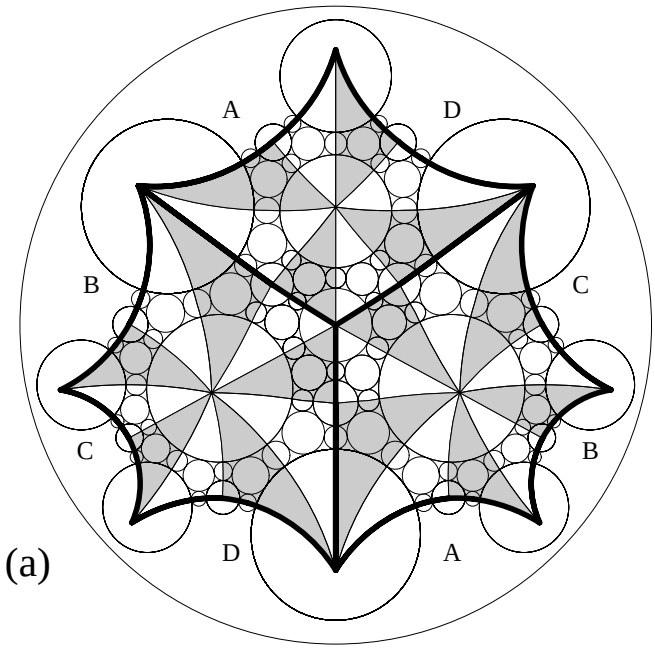

(a)

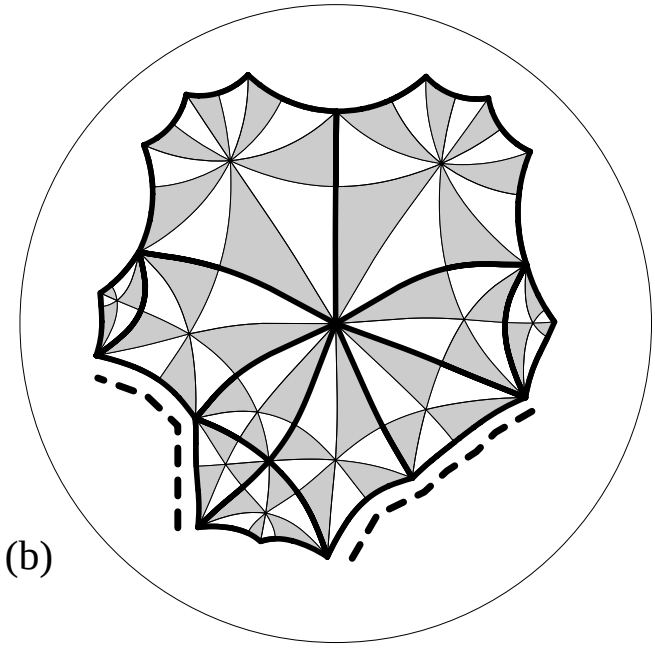

(b)

FIGURE 19. Dessins 8 and 9

highlights a central issue: *To what extent can one anticipate conformal implications directly from the combinatorics?*

5.4. **Higher Genera.** We begin with two very classical surfaces: the Klein "Hauptfigur" of [12] and the Picard curve. Historically, these resulted from other considerations, and only in hindsight are associated with "dessins". We also display a generic genus 4 dessin to show the level of complexity that our methods can handle. The main hurdle in preparing such examples lies in specifying the dessin combinatorics.

5.4.1. *Example 10.* Klein's "Hauptfigur" is a genus 3 surface which has played a seminal role in classical geometry and function theory. It is the **modular curve** $X(7)$ of degree seven and has an automorphism group of order $168 = 84(g-1)$, the maximal possible in genus $g = 3$. This curve also has an honored place in the visual history, thanks to the beautiful illustrations, now over a century old, produced for Klein.

Klein's surface R is the compact surface $\mathbb{H}/$, (7), where $\mathbb{H}$ is the upper half-plane and , (7) is the subgroup of $PSL(2,\mathbb{Z})$ consisting of elements congruent to $\pm id$ modulo 7. See, for example, [17, 22]. A natural triangulation G on R (which one can obtain geometrically, combinatorially, or *via* the group structure) is a 7-regular graph. A classical fundamental domain for R can be indentified within a tiling of the hyperbolic plane by equilateral hyperbolic triangles having angles $2\pi/7$.

We take (R, G) as our dessin; the circle packing (not shown) provides the image in Figure 20(a), an image familiar to analysts for more than a century. Figure 20(b) shows the associated dessin overlaying the carrier of the same circle packing. For the reader's benefit, this latter illustration indicates the side-pairings associated with the surface.

Note that the dessin faces of the dessin surface are *geodesic* $(2, 3, 7)$ triangles due to the ubiquitous symmetries of G. In particular, even with the coarse circle packing, these illustrations have perfect accuracy (up to the usual computational roundoff). It is because the dessin faces are geodesic triangles that this picture could be constructed a century ago — this will be in contrast to our next examples.

5.4.2. *Example 11.* Next is the genus 3 "Picard" curve $y^3 = x^4 - 1$. We first employ a dessin taken from Shabat and Voevodsky [30, p. 217]; this is pictured with the fundamental domain from the coarse packing in Figure 21(a).

The Picard curve can also be constructed by methods similar to Klein's surface, using the fact that it has a very rich automorphism group, one of order 48. In [26], J. R. Quine builds the fundamental domain of Figure 21(b) using $(2, 3, 12)$ triangles. The side-pairings are determined by labeling the sides counterclockwise, from 1 (as indicated) to 24; each even-numbered side k is then paired with side $k + 7$. It turns out that this triangulation arises from a dessin distinct from the one of Shabat and Voevodsky; the triangles forming the fundamental domain are rearranged in Figure 21(c) to more easily picture this alternate dessin. For the side-pairings, number the sides as before from 1 and identify each odd-numbered side k with side $k + 5$.

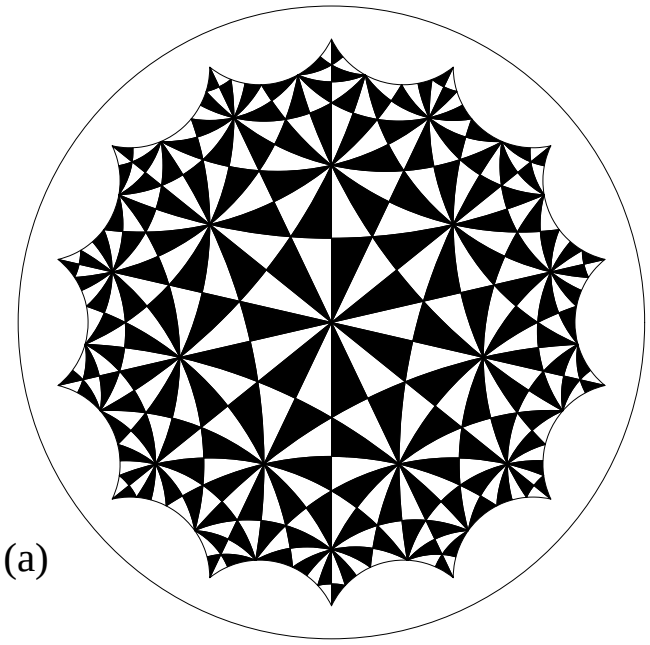

(a)

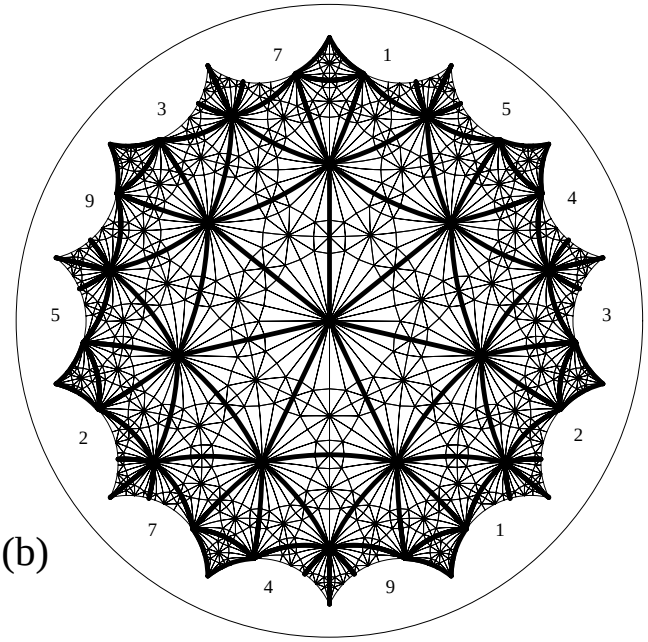

(b)

FIGURE 20. Klein's Hauptfigur

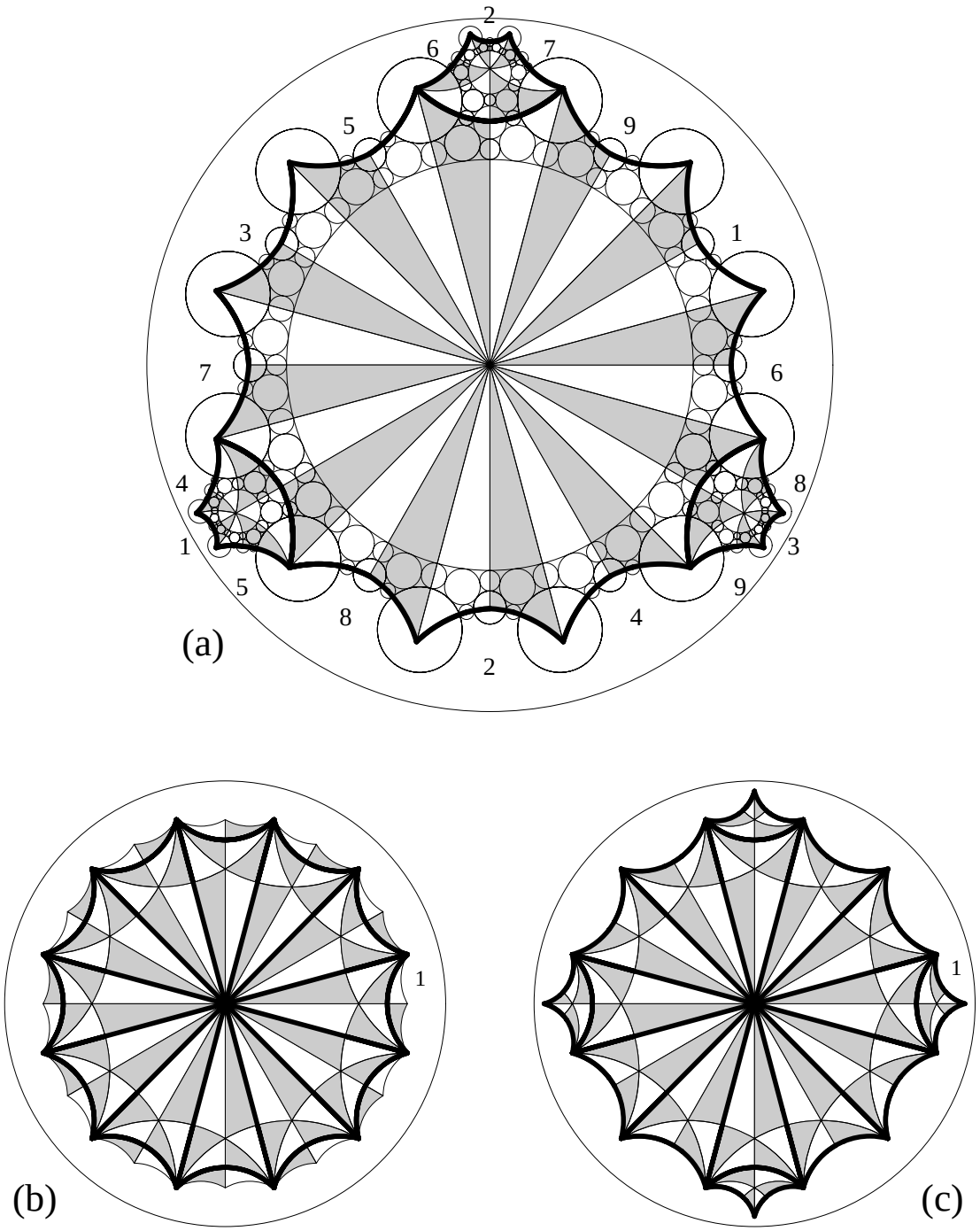

FIGURE 21. Two dessins for the Picard surface

It is convenient to have two genus 3 dessins determining the same conformal structure, since it affords us opportunities to judge the quality of circle packing approximations. (Is there some reason to anticipate this circumstance based solely on the combinatorics of the two dessins?) Comparing the triangulations, note that the triangles of Figure 21(b) (and (c)) are, as with the fundamental domain for Klein's surface in Figure 20(a), geodesic triangles, so this fundamental domain is essentially exact. On the other hand, the triangles of Figure 21(a) may appear to be geodesic, but in fact definitely are not. (One can see, for example, that in reflections of dessin faces across certain edges, the opposite angle on one side will be $\pi/12$, while that on the other is $\pi/4$.) The image of Figure 21(a), obtained from a coarse circle packing, is, as far as we know, only approximate.

5.4.3. *Example 12.* Our final example is a garden variety genus 4 dessin. The main difficulty with higher genera is largely that of encoding the combinatorics. Here we use the "pair of pants" paradigm.

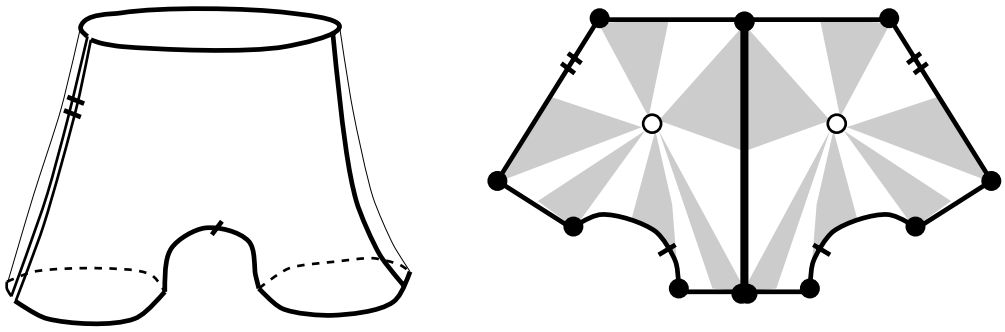

FIGURE 22. A standard pair of pants

A pair of pants is basically a sphere with three round discs removed; any compact hyperbolic Riemann surface can be decomposed as a disjoint union of a finite number of pairs of pants (with appropriate structure parameters) identified along boundary components. We will use the basic pair of pants shown in Figure 22, with conformal structure determined by two dessin-like 2-cells. A genus 4 surface constructed from 6 identical pairs of pants, twelve 2-cells, is shown in Figure 23.

Observe that at this point we have a highly symmetric surface, especially so since the particular pair of pants we are using has the greatest possible symmetry (only

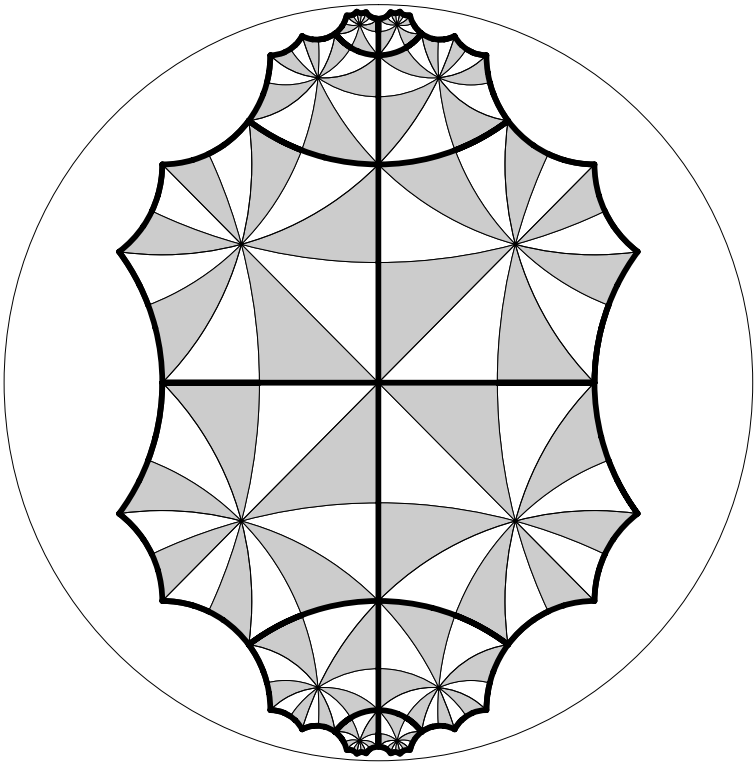

FIGURE 23. A symmetric genus 4 surface

countably many surfaces can be constructed from from copies of this pair). We have also built in some global symmetry for easy visualization. (One consequence is, as with Klein's surface, that the discrete conformal structure is precisely equal to the classical.)

We have modified the dessin by adding edges and vertices (see §6.1); the new fundamental domain from the coarse packing is shown in Figure 24. To help with visualization, modifications were restricted to the "upper" half of the dessin and left-right symmetry was maintained. A region of fine structure has also been blown up to show successive levels of detail.

This concludes our small Menagerie. Many additional examples could be given, both from the dessin literature and from other areas. There are, for example, the generalizations $\mathbb{H}/, (k)$ of Klein's surface for $k > 7$ and a plethora of pair-of-pants constructions. We move on to a discussion of some computational issues; see the Appendix for details on implementation.

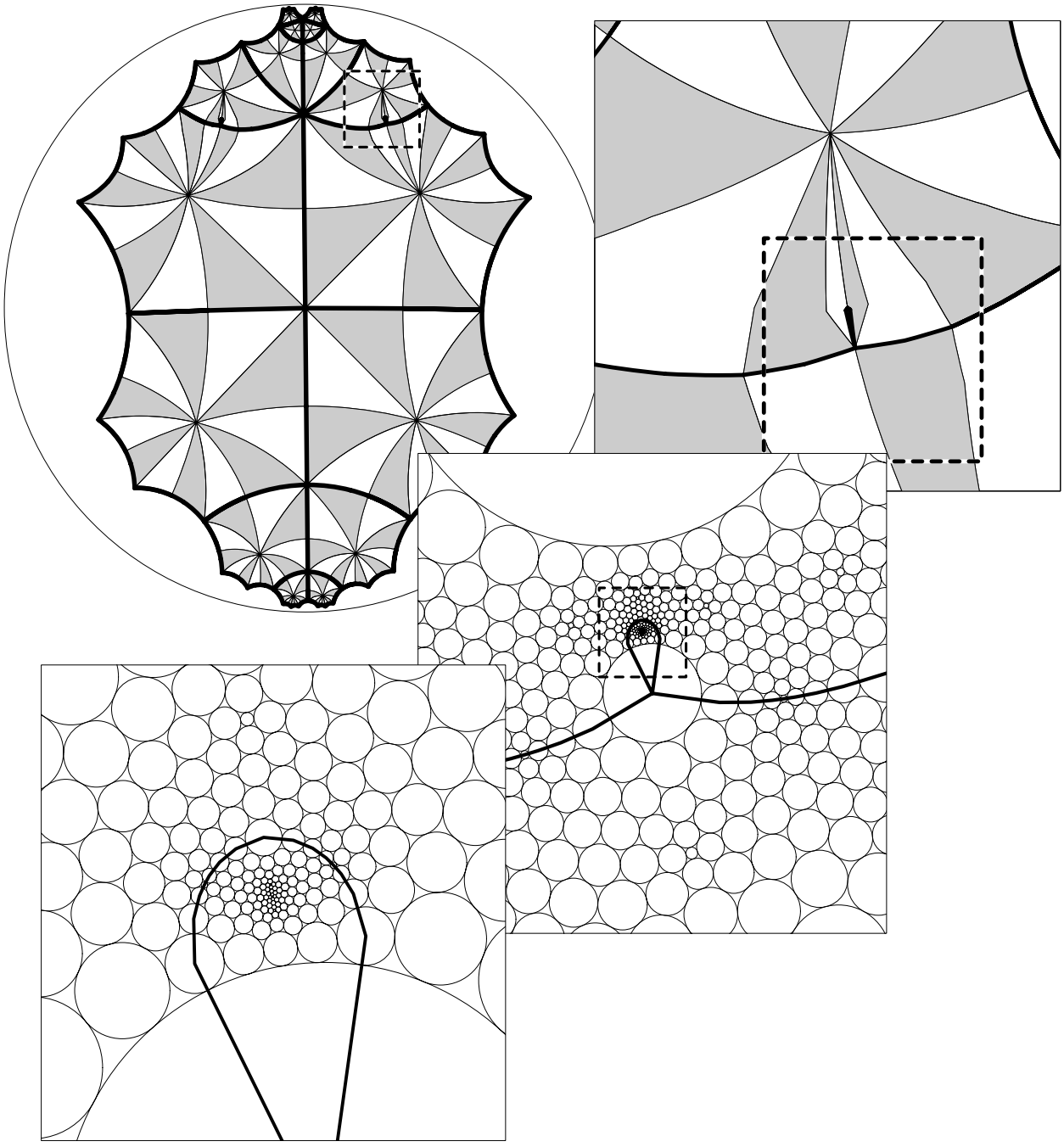

FIGURE 24. Details of a more generic genus 4 dessin

6. Computational Issues

The discrete theory of dessins based on circle packings — discrete conformal structures, discrete coverings, discrete Belyĭ maps, and so forth — is computationally accessible because there exist both theoretical and practical algorithms for computing circle packing radii in the various geometries. In other words, the discrete theory can be implemented and investigated experimentally. We would like to emphasize that experiments might provide classical insight both through analogy and through explicit approximation. Moreover, as we suggest in Section 7, the discrete theory has a certain charm of its own.

We must say to begin that we as yet have no firm quantitative handle on the internal consistency of circle packing structures nor on the accuracy with which they approximate the classical structures. Having said that, however, our experience suggests that *the discrete structures are internally very robust and remarkably close to the classical structures.* Our comments here will largely be directed to experimental observations (and potential observations) with Menagerie specimens. Comparisons to classical objects are, of course, complicated by the fact that few of them are known in any practical sense.

First we observe that quite complicated dessins can be circle packed with relative ease and appear to give visually consistent discrete structures (e.g. fundamental domains and Belyĭ maps). The main experimental hurdle typically lies in specifying the abstract combinatorics for the dessin (for which help is now available through the "dessin moves" described at the end of this section). From there, the experiments, carried out using `CirclePack` and `DesPack`, are fairly straightforward, modulo the usual laboratory glitches. (For more details on software, algorithms, implementation, run times, references, and so forth, see the Appendix.)

Recall that given a dessin (S, D) there is a countable collection of associated Belyĭ pairs: namely, the discrete pairs $(s_D^{(n)}, b_D^{(n)})$ for the various refinement stages and the classical pair (S_D, B_D) to which they converge (*per* Theorems 4.5, 4.8, and 4.10). We address mainly the case of positive genus g and consider the surfaces $s_D^{(n)}$ and S_D; when $g = 0$, roughly parallel considerations pertain to the Belyĭ maps. We may place the accuracy issues in three broad catagories: (I) How closely does a *computed* discrete conformal structure approximate the *actual* discrete conformal structure (given by the Circle Packing Theorem)? (II) How closely do the discrete conformal structures of successive refinements approximate one another? (III) How closely does the discrete conformal structure at a given stage approximate the classical conformal structure? We can try to tease some insight from our examples.

For issue I, Klein's surface, Example 10, with 336 dessin faces and a coarse packing involving 1004 circles, provides a particularly good starting place. Due to its order 168 automorphism group, the discrete conformal structures — at every level of refinement — are in theory precisely equal to its classical conformal structure, with dessin faces

which are geodesic $(2, 3, 7)$ triangles and a covering group which is (conjugate to) the modular group , (7). This gives several precise values to which one may compare computed ones.

Consider the coarse packing displayed in Figure 20. As discussed in the Appendix, the radii of the packing are computed so that the packing "angle sums" agree to approximately 10 digits with the value 2π; the radii are then used to lay out (a fundamental domain of) the packing. The ultimiate aim is accuracy in the placement of these circles. We carried out a few sample comparisons. (Incidently, the computation of this packing takes roughly 15 seconds on a Sparcstation 10.)

- Concerning the computed radii, note that symmetry implies that for each $i = 0, 1, \infty$, all the circles associated with i-vertices should share the same radius. Using repackings starting from randomized initial labels suggests that computed radii will agree to 7 digits.
- To judge accuracy in the placement of centers, we laid down circles to build the closed chain of 324 boundary faces in the fundamental domain of Figure 20. This process is akin to analytic continuation. It suggests accuracy to 5 digits in placing the boundary cusp points.
- Side-pairing maps represent key data for any covering and can be estimated from locations of boundary vertices of the fundamental domain. A simple check, for example, compares the hyperbolic distances between endpoints of identified sides; in Figure 20, these distances typically agree to 6 decimal places.

Further experiments should suggest how these various measures of accuracy respond to the error tolerances set in the packing routines. There are other highly symmetric cases in which the discrete and classical dessins are precisely equal, such as one form of Example 11 and the symmetric predecessor to Example 12 (Figure 24). However, we will not pursue this further here.

To address issue II, the stability of discrete structures under refinement, let us move to more generic examples. Consistency has certainly been one of the most striking features of the computer experiments: in example after example the discrete structures seem stable from the very first, coarsest packing. Figure 11 shows normalized discrete embeddings of the "one-armed" Dessin 4, from coarse through stage-4. The general shape seems reliable from the beginning, though the proportions of head and legs emerge more slowly. This is typical of our genus 0 experiments. In positive genus cases, both the salient features and the details seem to stabilize even more quickly.

For instance, let us return to the "peace" symbol of Example 7. We would expect (although we have no proof) that the surfaces $s_D^{(n)}$ from various stages are all distinct from one another and from S_D. In Figure 25, we have overlaid images of the boundaries of the fundamental regions for the coarse and for the stage-3 packings, respectively 82

and 5374 circles, and have enlarged the image of the cusp where they differ most; the euclidean distance between cusp points is approximately 0.003.

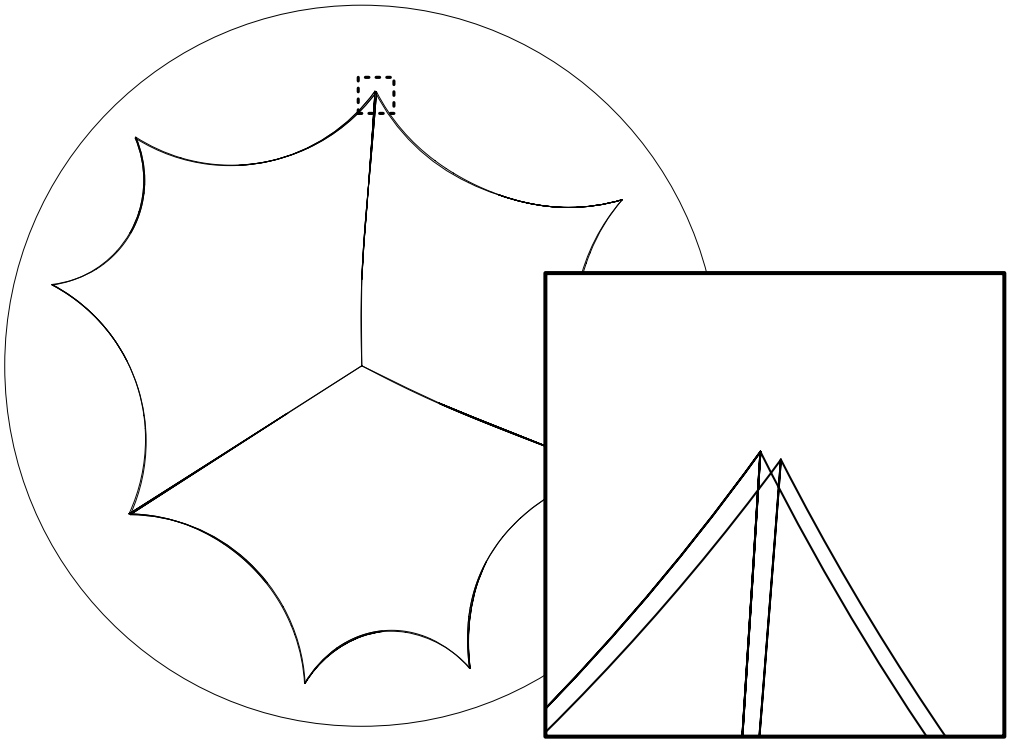

FIGURE 25. Comparing cusps for stages of Example 7

There is a point to be made about our discrete dessin drawings, particularly in genus zero. In a conformally correct dessin, the edges meeting at a vertex will meet with equal angles. In various of our illustrations of discrete dessins one can clearly see that this fails (e.g. Figure 2 or Figure 12). This is due, in part to our drawing method: dessins are drawn as piecewise geodesic arcs running through the centers of appropriate chains of circles. Accuracy would presumably improve if they were drawn as splines, with the requirement that they run through appropriate sequences of tangency points and come together at vertices with equal angles. This makes little difference in the positive genus cases. However, in spherical geometry, circle centers are not conformally determined (they are not preserved under Möbius transformations); tangency points are, and the use of splines can make noticable differences in dessin drawings. In any case, the pictures in the paper (and the package `CirclePack`) use the more computationally convenient circle centers.

Issue III concerns the accuracy of the descrete *vis-a-vis* the classical structures. The stability of the discrete conformal structures under refinement in conjunction with

Theorem 4.5 suggests some level of accuracy. Of course, further work needs to be done on the numerical side prior to any claims. Nonetheless, the Menagerie provides some opportunities to address accuracy beyond the very symmetric cases such as Klein.

In particular, the genus 1 dessin of Example 5 has been studied thoroughly and its classical j-function value was computed in [30, p. 215], namely:

$$4(8+3\sqrt{7})^2(2-\sqrt{7})^6(10-3\sqrt{7})^3 = 457208 - 172564\sqrt{7} \approx 646.5707574.$$

In Section 5, we gave numerical estimates of the complex modulus τ for the discrete torus at the coarse and at the stage-2 levels. We put these values through *Mathematica* to obtain the estimated j-function values, $j(\tau)$, with these results:

$$\text{Coarse stage: } 635.06238 - 0.00035i \qquad \text{Stage-2: } 642.57533 - 0.01011i,$$

representing errors of about 1.78 and 0.62 percent at the coarse and stage-2 levels, respectively.

Remark. The j-function itself may be constructed by a reflective process similar to Belyĭ maps, the only complication being that it has an infinite order ∞-vertex (a puncture) representing a logarithmic branch point; see [1]. Replacing the puncture by a vertex of high finite degree, one can theoretically construct discrete approximations to the j-function.

There are other opportunities to compare discrete and classical data, as with the tree of Example 4. We could also point to the interesting Picard surface, Example 11. In this instance we have two dessins which define the same surface. For one, the dessin faces are geodesic triangles, so as with the Klein surface, the discrete structures are all identical to the classical one. There seems no reason to expect this for the other dessin, so again one can compare the approximate structures to the known classical one.

The reader may have observed in our examples that circles associated with dessin vertices are often quite large, even in finer stages; one might be led to question the precision. This behavior, however, is wholly consistent with classical behavior. Recall that the number n of faces incident to a dessin vertex v is $2(b+1)$, where b is the order of the branch point B_D has at the point $z \in \mathbb{S}^2$ associated with v. If $b \geq 1$, B_D compresses large neighborhoods about z into small neighborhoods about $B_D(z)$. In other words, B_D is approximately constant on a large neighborhood of z. This, rather than any loss of precision, is what the large circle at v reflects for the discrete mapping.

The question of theoretical accuracy — how closely the discrete conformal structures (resp. discrete Belyĭ maps) for a dessin approximate the classical conformal structures (resp. classical Beylĭ maps) seems to be very deep. As we point out in the final section, approximation is not the only legitimate aim for studying the discrete structures.

6.1. **Dessin Modifications.** There is a small number of elementary **dessin moves**, reminiscent of Reidemeister moves in knot diagrams, which allow one to construct an arbitrary dessin on a compact surface from any beginning dessin. This is not difficult to

establish, and the reader can furnish the details. We mention this because these dessin moves are now not only *practical* in the experimental setting, but almost *essential*. Nearly all of our more complicated dessins have been built from simple seeds by dessin moves which added complexity. In turn, the fact that moves can be implemented opens a new avenue for thinking about dessin structures and their relations to one another.

The basic dessin moves are of three types: (I) adding/deleting vertices, (II) adding/deleting free edges, and (III) adding/deleting separating edges. Recall that dessins are connected and 2-colorable graphs, and the moves must preserve this. So, for example, a type I move adding a vertex actually requires adding two vertices. With this caviat, the moves are largely self-explanatory. It is also useful, particularly working in the category of clean dessins, to identify common "composite" moves, such as adding a double free edge or a loop at a 0-vertex, or adding a "bridge" across a 2-cell from one 0-vertex to another. Only the add versions of these composite moves have been implemented in `DesPack` so far, and these were used in creating the Menagerie.

Concrete examples of moves are illustrated in Figure 26. We started with the simplest genus 1 dessin, two loops at a base point, and applied a sequence of "composite" moves leading to Dessin 6, the lower right hand figure. The coarse dessin, circle packing, and shaded dessin faces are shown at various intermediate stages, all normalized to place the bottom corner circles at 0 and 1.

When D' is obtained from the dessin D by a finite sequence of dessin moves, each of which is an "adding" move as opposed to a "deleting" move, we call D' a **dessin refinement** of D.

Proposition 6.1. *Any two dessins D and D' on an oriented closed surface S share a common refinement.*

The proof is left to the reader. It helps to note that by applying a small isotopy to D', one may assume that D and D' are in general position. Their union may then be converted into a 2-colorable graph of which they are both refinements. A corollary to this proposition is: *On a topological surface S, any dessin D' may be obtained from any other dessin D by a finite sequence of elementary dessin moves.*

6.2. **Graph Embedding.** The carrier of a univalent circle packing in a surface provides an embedding of its complex $\mathcal{K}$ (in fact, in the cases we have been considering, it even provides the geometry for the surface). In some cases it may not be the surface which is of interest, but rather the embedding of the 1-skeleton $\mathcal{K}^{(1)}$ as a graph. Indeed, circle packings are valuable for embedding fairly general locally planar graphs: the 1-skeletons of their carriers are geodesic, they can simultaneously provide geodesic dual orthogonal graphs, and graph edges meet at angles bounded below by constants depending only on degree. Graphs of considerable complexity can be generated automatically and randomly and the packings computed relatively quickly; packing algorithms are known that work in polynomial time with the number of vertices.

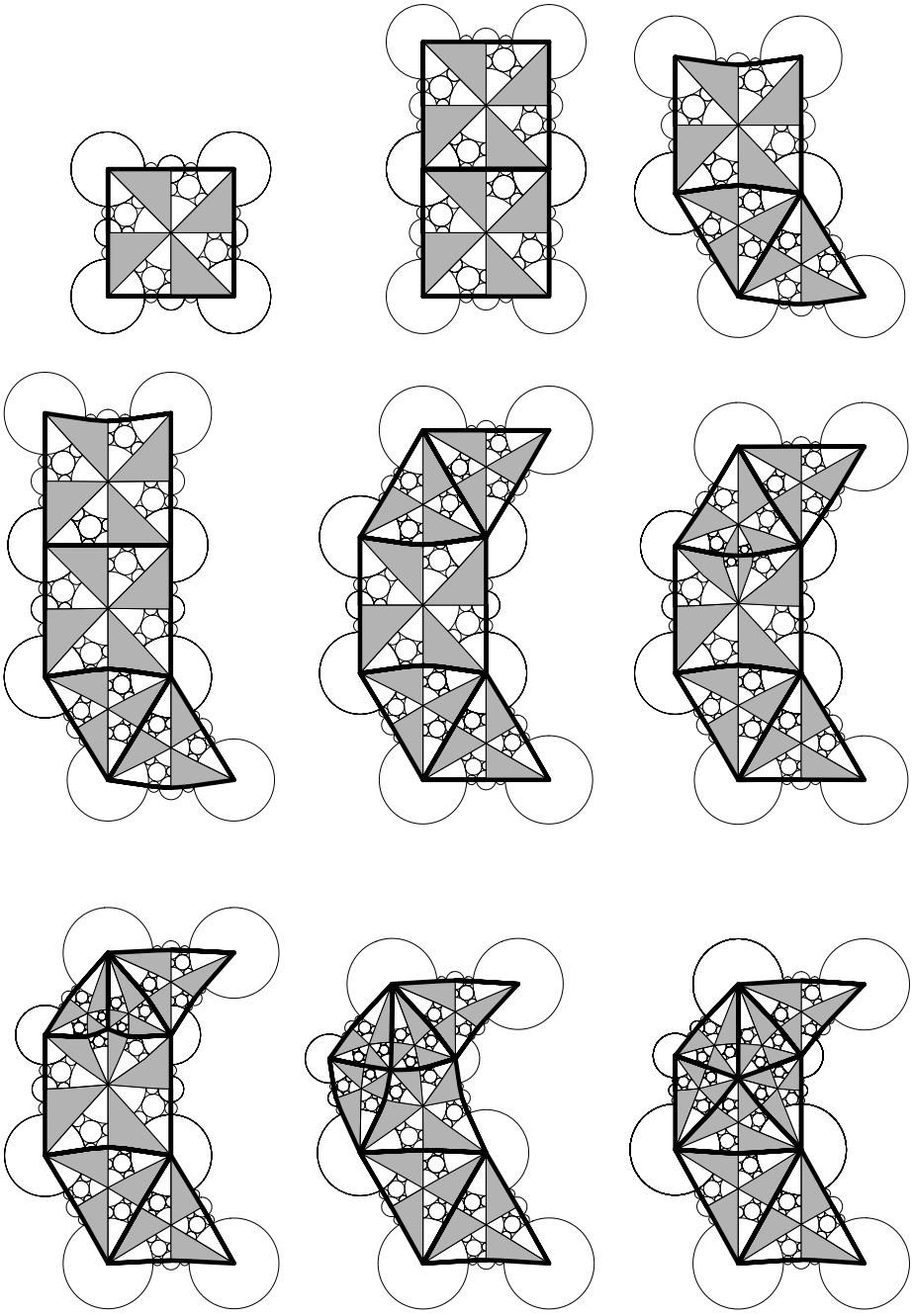

FIGURE 26. Dessin moves generating Dessin 6

The circle packing techniques of the paper provide embeddings of general triangulated surfaces, polygonal surfaces, open and bordered surfaces, and are being applied in recent work on conformal "tilings" (see [6]). Circle packings tend to be accompanied in all these settings by vestiges of classical analysis — random walks, discrete Laplacians, discrete extremal length, discrete analytic functions, and so forth.

Some of the interest in dessins d'enfants stems from fact that they provide a countably dense set of points of Teichmüller space (see the next section), and that these points follow an underlying organizational structure. Physicists, for instance, are interested in statistical and asymptotic analysis of surfaces.

7. The Discrete Option

Circle packing theories have displayed a remarkable knack for both mimicking and approximating their continuous models in various areas of conformal geometry and analytic function theory. It might be said that they provide a "quantum theory which is classical in the limit". We wish to close by formulating some of the open issues in the dessin setting. In particular, we would suggest a broad and somewhat independent view of the discrete theory, since it has attractions and raises questions of its own.

With regard to *approximating* the classical theory, it seems that the discrete theory has the potential to contribute in several ways; visualization, manipulation, dessin modification, and rough numerical estimation. Its main strength seems to lie in the experimental setting which it provides for developing intuition and perhaps new theoretical insights. It is not yet suitable for highly accurate numerical approximations (as are available, e.g., with trees [9]) and there is considerable work to be done on theoretical accuracy, numerical precision, and rates of convergence. There is a rapid rise in computation times with successive refinement, and even with numerical improvements one might wonder about the long range practicality for actual estimation. This is somewhat counterbalanced, however, by the surprising accuracy of even coarse packings; this accuracy is one of the more intriguing issues *vis-a-vis* the classical theory. Questions such as the Teichmüller distance from S_D to s_D are of considerable interest, but probably very hard to pin down, even for individual dessins. Despite any current numerical limitations, however, note that circle packing is the only game in town for approximating most conformal structures.

However, we want to leave these issues for a moment and move our thinking to the discrete setting — after all, the qualitative features of the theory seem essentially unchanged. *Suppose you were resigned to living entirely in the* ***discrete world***. What would you see as the key *intrinsic* issues? What internal structures do the collections of surfaces and functions have? fail to have? How much algrebraic structure can one see? What can one learn when your computer can actually build surfaces?

To frame some of the discussion, we might consider dessins of a fixed positive genus g as viewed from the standpoint of the Teichmüller space Teich(g). On the discrete side,

we will restrict attention to the "course" dessin surfaces only — foregoing refinements. Belyĭ 's theorem and the density of algebraic numbers in the complex field imply that the set of (classical) dessin surfaces

$$\mathrm{T}^*(g) = \{S_D : \mathrm{genus}(D) = g\} \subset \mathrm{Teich}(g)$$

form a countable dense subset. Indeed, these surfaces are characterized as those having defining equations with coefficients in a number field. This is one of their principal attractions; they provide a geometric playground for the study of algebraic numbers and Galois groups.

There is now a parallel collection of discrete (coarse) dessin surfaces, which we will denote by

$$\mathrm{t}^*(g) = \{s_D : \mathrm{genus}(D) = g\} \subset \mathrm{Teich}(g).$$

This provides new playground equipment.

There are many natural questions about $\mathrm{t}^*(g)$. Note that it intersects $\mathrm{T}^*(g)$, as with the Klein surface (e.g., in the presence of sufficient symmetry, see Example 10). Are their any other intersections? Intuition suggests that these sets are essentially disjoint. Are there redundancies in $\mathrm{t}^*(g)$, in the absence of symmetry? Within $\mathrm{T}^*(g)$ there are systemic redundancies: for instance, the 1-skeleton of $\mathcal{T}(D)$, treated as a graph, leads to a new dessin D', but Proposition 4.1 implies that $S_D = S_{D'}$. Other redundancies are perhaps much deeper, as with the distinct dessins yielding the Picard surface of Example 11. (Incidently, with modifications of the proof of Theorem 4.5, one can prove that $\mathrm{t}^*(g)$ is a countable dense set in $\mathrm{Teich}(g)$; see also [7].)

A quite fascinating open question concerns the characterization of the points of $\mathrm{t}^*(g)$. Here there is a tantalizing new connection to algebraic numbers proven by McCaughan [24]: *The covering group for a point of* $\mathrm{t}^*(g)$ *is conjugate to a subgroup of* $\mathrm{PSL}(2, \overline{\mathbb{Q}})$ *(resp.* $\mathrm{PSL}(2, \overline{\mathbb{Q}} + i\overline{\mathbb{Q}})$*) if* $g > 1$ *(resp.* $g = 1$*).* That is, one may choose the covering group so that its matrix representatives have algebraic entries. For example, in the genus 1 cases, the modulus will be algebraic.

The ability in the discrete setting to experiment with quite complicated dessins suggests new issues. What, for example, are the algebraic implications of dessin modification? Are there geometric descriptions of dessin Galois orbits, or is this truely an algebraic notion? Can one actually do arithmetic with surfaces? Just how suitable is this new playground equipment if you are interested in number fields and Galois theory?

Some of the interest in dessins d'enfants, in string theory, for instance, stems largely from the fact that dessins impose an "organizing principle" on the space of surfaces through the dense sets $\mathrm{T}^*(g)$. The discrete theory may offer definite advantages. Surfaces of considerable complexity can be generated automatically and randomly and the packings computed (at least at the coarse stage) relatively quickly, aiding in the statistical and asymptotic analysis of surfaces. Circle packings seem to provide a natural

geometry of the type that nature might favor, and their refinements are akin to the physicist's renormalization.

In closing, the authors might suggest staying in this discrete world for a while longer — it has much of the geometry, combinatorics, and even possibly the number theory of the classical setting, plus a certain charm all its own.

8. Appendix: Implementation

The examples of the paper were produced using two suites of computer programs: `CirclePack`, a graphically based program for creating, computing, manipulating, and displaying circle packings, and `DesPack`, a set of auxiliary programs for building dessins and their associated data structures. These programs are available for use by others from the second author.

8.1. **A Quick Experiment.** As an overview, let us follow a typical development cycle for a dessin, say the genus 2 dessin of Example 7.

1. Start with the common fundamental domain for a genus 2 surface, schematically an octagon with "normal form" side-pairings. This is the minimal dessin of genus 2 and its canonical triangulation involves 16 triangles. These are numbered and the adjacency relationships are entered in an ASCII file (in a straightforward format) as input to `DesPack`. This file contains what we will informally refer to as a "red" chain, a chain of faces enclosing a fundamental region.

2. `DesPack` is programmed with the composite dessin moves of §6.1; three of these convert the basic dessin into the dessin D of Figure 17.

3. `DesPack` now generates a simple ASCII file representing a 2-complex $\mathcal{K}$ which encodes the combinatorics of the coarse circle packing for D. It also produces a list of faces of $\mathcal{K}$ enclosing a fundamental domain and it specifies the requisite geometry, in this case, hyperbolic.

4. `CirclePack` reads the combinatorics $\mathcal{K}$ and computes the associated hyperbolic packing label. This is a crucial step: theory gives the surface s_D. In practice, this is represented as a unique "packing label" for $\mathcal{K}$ consisting of the hyperbolic radii for $P_{\mathcal{K}}$. `CirclePack` computes the packing label using a modification of an iterative algorithm suggested by Thurston, an algorithm which has been proven to converge [4].

5. Using the hyperbolic radii, combinatorics, and red chain of the packing, `CirclePack` will lay out a configuration P of circles in the hyperbolic plane whose carrier is the desired fundamental domain of the covering of s_D.

6. `DesPack` and `CirclePack` can communicate to permit display of various information in the hyperbolic plane: e.g., drawing the dessin, shading faces, labeling the 0- 1- and ∞-points, etc.

7. `CirclePack` will generate the combinatorics $\mathcal{K}_n$ for one (or more) hexagonal refinements of the packing for $\mathcal{K}$. It can then compute the packing label for the refined combinatorics, lay out the new fundamental domain, and in conjunction with `DesPack`, carry out various drawing operations.

The difficulty in building examples typically lies in specifying dessin combinatorics and a red chain for visual layout. With this in hand, the remaining operations are quite fast. The sequence of commands to `CirclePack` is typically entered in a "script" file, which can be shared with others and invoked automatically.

8.2. **The algorithm.** The most computationally intense stage in working with discrete dessins involves computation of packing radii for circle packing complexes $\mathcal{K}$. The "packing" algorithm in `CirclePack` is iterative, similar in spirit to classical ralaxation methods for solving the discrete Laplace equation: the routine repeatedly passes through the list of circles, adjusting the radius of each circle it visits to make it fit with its immediate neighbors. The algorithm is described briefly in [10, p. 316]; for additional details and recent improvements in implementation due to Chuck Collins, see [8].

The computation times increase rapidly with the number of circles and the desired numerical accuracy. Tables 1 and 2 list the timings for several stages of most of our examples. The "Iterations" refers to number of passes through the full set of vertices, so its product with the previous column indicates the total number of radii adjustments in the iterative repacking algorithm. The runs were carried out on DEC AlphaStation 5/333 machine. The timings indicate CPU time for the repacking phase only, disregarding overhead, such as input/output. They were measured in seconds, so "0" in the last column indicates a repacking time of less than a second. Note that even the most complex course packings required less than a second to pack.

The examples in the table represent roughly 9 digit accuracy. To suggest the effect of desired accuracy, Table 3 lists timings for the stage-3 Klein surface (64,508 circles) for tolerances set from 10^{-5} down to 10^{-10}.

The properties of packing labels and the behavior of the packing algorithm are quite fascinating in their own right, and significant improvements may be possible with deeper understanding. For instance, radii adjustments may be modeled as discrete Markov processes having to do with the flow of "curvature" among vertices in the packing complex; see [32] and [31]. Packings of refinements, important if one wishes to approximate the classical objects, may be improved through multi-grid methods in which the labels for coarser packings provide the initial guesses for labels of their refinements; see [10, §5]. Finally, the algorithms are amenable to significant parallelization.

Example # Genus	Refinement Stage	Circle count	Iterations	CPU time (min. m, sec. s)
Ex.#2, $g = 0$	coarse	25	31	0
(lollypop)	1	97	66	0
	2	385	319	0
	3	1537	1325	10s
	4	6145	5017	2m 33s
Ex.#3, $g = 0$	coarse	74	27	0
(one-arm)	1	290	68	0
	2	1154	251	1s
	3	4610	1234	32s
	4	18434	5019	9m 15s
Ex.#4, $g = 0$	coarse	109	11	0
(tree)	1	433	36	0
	2	1729	104	1s
	3	6913	524	21s
	4	27650	2158	6m 15s
Ex.#5, $g = 1$	coarse	144	41	0
($\sqrt{7}$)	1	576	94	0
	2	2304	213	2s
	3	9216	580	26s
	4	36864	1656	5m 16s
Ex.#6, $g = 1$	coarse	144	55	0
($\sqrt{7}$-conj.)	1	576	171	0
	2	2304	389	4s
	3	9216	1083	50s
	4	36864	3374	11m 04s

TABLE 1. Computation times, genus 0 and 1

8.3. **Accuracy.** In Section 6 we gave some numerical results from our examples to suggest the accuracy of the discrete methods. Recall that this involved both computational and theoretical accuracy issues.

As for computational accuracy, consider a given circle packing complex $\mathcal{K}$ triangulating a compact surface. The associated packing label is effectively computable, meaning that in theory the packing algorithm can produce an approximation to the packing label having any desired level of accuracy. In addition, geometric considerations and certain monotonicity properties associated with circle configurations provide upper estimates on the errors.

In practice, the accuracy of computed packing labels is inferred from the accuracy of "angle sums". The angle sum at a vertex v is the sum of the angles in the faces to which v belongs; each of these angles is computed from the law of cosines using the

Example # Genus	Refinement Stage	Circle count	Iterations	CPU time (min. m, sec. s)
Ex.#7, $g = 2$	coarse	82	36	0
(peace)	1	334	98	0
	2	1342	325	2s
	3	5374	1273	38s
	4	21502	4004	7m 54s
Ex.#8, $g = 2$	coarse	82	36	0
(peace 2)	1	334	108	0
	2	1342	346	2s
	3	5374	1100	33s
	4	21502	4568	9m 27s
Ex.#9, $g = 2$	coarse	250	96	0
(generic)	1	1006	332	1s
	2	4030	1146	25s
	3	16126	4234	6m 37s
Ex.#10, $g = 3$	coarse	1004	110	0
(Klein)	1	4028	406	9s
	2	16124	1544	2m 14s
	3	64508	4776	32m 18s
Ex.#11, $g = 3$	coarse	284	49	0
(Picard:	1	1148	146	0
Quine)	2	4604	494	12s
	3	18428	1724	3m 8s
	4	73724	6049	46m 11s
Ex.#11, $g = 3$	coarse	140	34	0
(Picard:	1	572	73	0
Sabbat &	2	2300	261	3s
Voevodsky)	3	9212	1048	55s
	4	36860	3486	12m 23s
Ex.#12, $g = 4$	coarse	522	94	0
(generic)	1	2106	248	3s
	2	8442	952	46s
	3	33786	3238	11m 27s

TABLE 2. Computation times, higher genus

labels for v and the other two vertices. It measures how close the immediate neighbors come to wrapping round v.

Inaccuracies also arises when the circle packing (or its fundamental domain) is actually laid out on the plane, the disc, or sphere (which is actually projected from the disc). Due to inevitable errors in computed radii, there is no consistent way to lay down an associated configuration of circles meeting the requisite tangency pattern. In practice, the circle centers are computed sequentially in successive generations from an

Tolerance	10^{-5}	10^{-6}	10^{-7}	10^{-8}	10^{-9}	10^{-10}
Iterations	1100	1978	2576	3422	4033	4776
CPU time	7m 13s	13m 19s	17m 20s	23m 14s	27m 6s	32m 18s

TABLE 3. Effect of tolerance in stage-3 Klein surface times

initial circle; errors frequently tend to cancel one another, and an essentially consistent packing generally emerges. When errors are too large, fissures occur in the pattern as artifacts of the plotting sequence and one typically sends the radii through the packing routines with a smaller error tolerance. (The tables above reflect 10 decimal place accuracy, though 5 places will generally yield a coherent packing.)

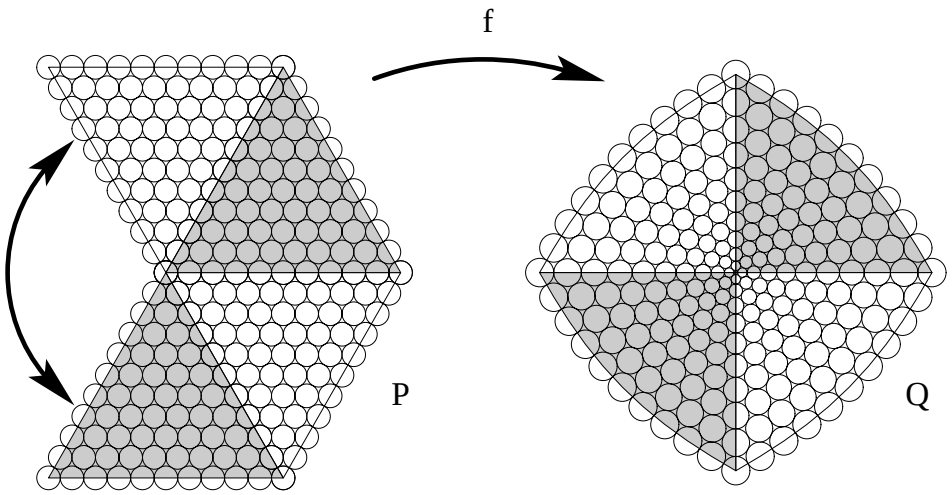

FIGURE 27. A discrete power map

8.4. **Cone Points.** We conclude by looking at discrete power maps. When d faces meet at a vertex v of an equilateral surface, forming a "cone point", the local coordinate chart at v is the power map $\phi : z \mapsto z^{6/d}$. Discrete structures mimic this behavior, as Figure 27 illustrates with $d = 4$. The packings P and Q have the same combinatorics. The radii of P prevent it from embedding in the plane, hence the arrow indicating a missing attachment. A packing operation leads to Q; the circles have been forced to change sizes in order to flatten out at v. The circle packing map $f : P \longrightarrow Q$ is the discrete analogue of $z \mapsto z^{6/d}$. In fact, with successive refinements (and appropriate

normalizations), refined maps f_n will converge to ϕ. The "repacking" algorithm is where the combinatorics and the geometry debate with one another to achieve an embedding.

References

1. Tom M. Apostol, *Modular functions and Dirichlet series in number theory*, 2nd ed., Springer Verlag, New York, 1990.
2. Michel Bauer and Claude Itzykson, *Triangulations*, The Grothendieck Theory of Dessins d'Enfants (Leila Schneps, ed.), London Math. Soc. Lecture Note Series, vol. 200, Cambridge Univ. Press, Cambridge, 1994, pp. 179–236.
3. A. F. Beardon, *A primer on Riemann surfaces*, London Math. Soc. Lecture Note Series, vol. 78, Cambridge University Press, Cambridge, 1984.
4. Alan F. Beardon and Kenneth Stephenson, *The uniformization theorem for circle packings*, Indiana Univ. Math. J. **39** (1990), 1383–1425.
5. Lipman Bers, *Finite dimensional Teichmüller spaces and generalizations*, Bull. AMS **5** (1981), 131–172.
6. Philip L. Bowers and Kenneth Stephenson, *A regular pentagonal tiling of the plane*, Conformal Geometry and Dynamics, to appear.
7. ———, *Circle packings in surfaces of finite type: An in situ approach with application to moduli*, Topology **32** (1993), 157–183.
8. Chuck Collins and Kenneth Stephenson, *A circle packing algorithm*, preprint.
9. Jean-Marc Couveignes and Louis Granboulan, *Dessins from a geometric point of view*, The Grothendieck Theory of Dessins d'Enfants (Leila Schneps, ed.), London Math. Soc. Lecture Note Series, vol. 200, Cambridge Univ. Press, Cambridge, 1994, pp. 79–113.
10. Tomasz Dubejko and Kenneth Stephenson, *Circle packing: Experiments in discrete analytic function theory*, Experimental Mathematics **4** (1995), no. 4, 307–348.
11. Hershel M. Farkas and Irwin Kra, *Riemann surfaces*, Graduate Texts in Math, vol. 71, Springer-Verlag, New York, 1980.
12. Robert Fricke and Felix Klein, *Vorlesungen über die Theorie der automorphen Functionen*, vol. I and II, B. G. Teubner, 1897-1912.
13. A. Grothendieck, *Esquisse d'un programme*, (1985), Preprint: introduced Dessins.
14. Zheng-Xu He and Oded Schramm, *On the convergence of circle packings to the Riemann map*, Invent. Math. **125** (1996), 285–305.
15. G. A. Jones and M. Streit, *Galois groups, monodromy groups and cartographic groups*, preprint.
16. Gareth A. Jones, *Graph embeddings and maps on surfaces 1*, Mathematica Slovaca **47** (1997), no. 1, 1–33.
17. F. Klein and R. Fricke, *Vorlesungen über die Theorie der elliptischen Modulfunctionen, vol. 1, 2*, Tuebner, Leipzig, 1890.
18. S. Kravetz, *On the geometry of Teichmüller spaces and the structure of their modular groups*, Ann. Acad. Sci. Fenn. **A1278** (1959), 1–35.
19. O. Lehto and K. I. Virtanen, *Quasiconformal mappings in the plane*, 2nd ed., Springer-Verlag, New York, 1973.
20. Olli Lehto, *Univalent functions and Teichmuller spaces*, Springer-Verlag, New York, 1987.
21. M. Linch, *A comparison of metrics on Teichmüller space*, Proc. AMS **43** (1974), 349–352.
22. Wilhelm Magnus, *Noneuclidean tesselations and their groups*, Academic Press, New York, London, 1974.
23. Howard Masur, *On a class of geodesics in Teichmüller space*, Annals of Math. **102** (1975), no. 2, 205–221.

24. G. J. McCaughan, *Some topics in circle packing*, Ph.D. thesis, University of Cambridge (advisor: Keith Carne), 1996.
25. Subhashis Nag, *The complex analytic theory of Teichmüller spaces*, Canadian Mathematical Society Series of Monographs and Advanced Texts, Wiley-Interscience, John Wiley and Sons, New York, 1988.
26. J. R. Quine, *Jacobian of the Picard curve*, Extremal Riemann surfaces, Contemporary Math, vol. 201, Amer. Math. Soc., Providence, 1997, pp. 33–41.
27. John G. Ratcliffe, *Foundations of hyperbolic manifolds*, Graduate Texts in Math, vol. 149, Springer-Verlag, New York, Heidelberg, Berlin, 1994.
28. Burt Rodin and Dennis Sullivan, *The convergence of circle packings to the Riemann mapping*, J. Differential Geometry **26** (1987), 349–360.
29. L. Schneps (ed.), *The Grothendieck theory of dessins d'enfants*, London Math. Soc. Lecture Note Series, vol. 200, Cambridge Univ. Press, Cambridge, 1994.
30. G. B. Shabat and V. A. Voevodsky, *Drawing curves over number fields*, The Grothendieck Festschrift, Vol. III (Boston, MA), Birkhauser Boston, 1990, pp. 199–227.
31. Kenneth Stephenson, *A probabilistic proof of Thurston's conjecture on circle packings*, Rendiconti del Seminario Mate. e Fisico di Milano, to appear.
32. ———, *Circle packings in the approximation of conformal mappings*, Bulletin, Amer. Math. Soc. (Research Announcements) **23, no. 2** (1990), 407–415.
33. William Thurston, *The geometry and topology of 3-manifolds*, Princeton University Notes, preprint.
34. ———, *The finite Riemann mapping theorem*, 1985, Invited talk, An International Symposium at Purdue University on the occasion of the proof of the Bieberbach conjecture, March 1985.
35. Joseph A. Wolf, *Spaces of constant curvature*, Publish or Perish Inc., Wilmington, DL, 1984.
36. Jürgen Wolfart, *Mirror-invariant triangulations of Riemann surfaces, triangle groups, and Grothendieck dessins. variations on a theme of Belyi*, (1992), Frankfurt Preprint.

Florida State University
E-mail address: bowers@gauss.math.fsu.edu

University of Tennessee, Knoxville
E-mail address: kens@math.utk.edu